MECHANICAL ANALYSIS OF CORRUGATED STEEL PIPE WITH DIFFERENT CRYOGENIC FLUIDS

M.Tech Dissertation

By

Syed Mahaboob Idris

(11300829)

DEPARTMENT OF MECHANICAL ENGINEERING

LOVELY PROFESSIONAL UNIVERSITY

PHAGWARA, PUNJAB (INDIA) -144411

2014- 2015

MECHANICAL ANALYSIS OF CORRUGATED STEEL PIPE WITH DIFFERENT CRYOGENIC FLUIDS

DISSERTATION-II

Submitted in Partial Fulfilment of the

Requirement for Award of the Degree

Of

MASTER OF TECHNOLOGY

In

MECHANICAL ENGINEERING

By

SYED MAHABOOB IDRIS

(11300829)

Under the Guidance of

Mr GAURAV VYAS

DEPARTMENT OF MECHANICAL ENGINEERING

LOVELY PROFESSIONAL UNIVERSITY

PHAGWARA, PUNJAB (INDIA) -144411

2014-15

MECHANICAL ANALYSIS OF CORRUGATED STEEL PIPE WITH DIFFERENT CRYOGENIC FLUIDS

DISSERTATION-II

Submitted in Partial Fulfilment of the

Requirement for Award of the Degree

Of

MASTER OF TECHNOLOGY

In

MECHANICAL ENGINEERING

By

SYED MAHABOOB IDRIS

(11300829)

Under the Guidance of

Mr GAURAV VYAS

DEPARTMENT OF MECHANICAL ENGINEERING

LOVELY PROFESSIONAL UNIVERSITY

PHAGWARA, PUNJAB (INDIA) -144411

2014-15

Lovely Professional University, Jalandhar, Punjab

CERTIFICATE

I hereby certify that the work which is being presented in the dissertation entitled **"Mechanical analysis of corrugated steel pipe with different cryogenic fluids"** in partial fulfilment of the requirement for the award of degree of **Master of Technology** and submitted in Department of Mechanical Engineering, Lovely Professional University, Punjab is an authentic record of my own work carried out during period of Dissertation under the supervision of **Mr Gaurav Vyas**, **Assistant Professor**, Department of Mechanical Engineering, Lovely Professional University, Punjab.

The matter presented in this dissertation has not been submitted by me anywhere for the award of any other degree or to any other institute.

Date: **Syed Mahaboob Idris**

This is to certify that the above statement made by the candidate is correct to best of my knowledge.

Date: **Mr Gaurav Vyas**

Supervisor

The M- Tech Dissertation examination of Syed Mahaboob Idris, has been held on _____

Signature of Examiner

ACKNOWLEDGEMENT

I am deeply indebted to my dissertation advisors, Assist Prof. Raja Sekhar Dondapati, Assist Prof. Gaurav Vyas for their respectable guidance, support and encouragement. This dissertation would not have been accomplished without their valuable advices and thoughts.

I am grateful to Mrs Preeti Rao Usurumarti for her guidance during my whole dissertation work. I would like to thank to Dr Rajiv Kumar Sharma (Head of Thermal Engineering Department), Dr Amit (Head of Manufacturing Department) and Mr Gurpreet Singh Phull (Head of Design Engineering Department) for their priceless support.

I would also like to thank Mr Barjinder Singh Bedi, Mr Ankur Bahl, Mr Dilbaj Singh, Mr Minesh Vohra, Mr Aashish Sharma, Ms Garima, Mr Varun Goyal, Mr Harpal Singh, Mr P. Narasimha Vinod, Mr Pyuesh Gulati, Mr Ankit Sharma and Mr Vijay Shankar for their intense support in developing my thesis to the present stage.

I am also grateful to my research team members Mr Abhinav Kumar, Mr Jeswanth Ravula, Mr Aal Arif Sarkar, Mr Mohit Kalsia, Mr Shivam S Verma, Mr Ajay Kumar Ramani, Mr S. Mugilan, Mr. U. Venkataramana, Mr G. Rajesh, Mr Balakrishna pandian who have helped me during my short period of association with them and friends Mr Sumit Saini, Mr B.Pavan Kumar who indirectly supported gave their valuable support and suggestions.

Last but not the least, my special gratitude and love go to my parents for their endless love, support and encouragement throughout my life. Acknowledging the parents support would be the foremost in achieving what I am now.

Syed Mahaboob Idris

NOMENCLATURE

P	Pressure
P_c	Critical Pressure
T	Temperature
T_c	Critical Temperature
H	Magnetic Field
H_c	Critical Magnetic Field
HTS	High Temperature Superconductor
SCN	Super Critical Nitrogen
SCAR	Super Critical Argon
SCH	Super Critical Hydrogen
CSP	Corrugated Steel Pipe
SCO	Super Critical Oxygen
LTS	Low Temperature Superconductor
SS316LN	Stainless steel pipe
DC	Direct current
FEM	Finite element method
LN_2	Liquid Nitrogen
C-Type	Circular corrugation type
R-Type	Rectangular corrugation type
T-Type	Triangular corrugation type

ABSTRACT

The losses encountered while transmitting power can be reduced drastically by using high temperature superconducting (HTS) cables. However in retaining the superconductivity the coolants such as supercritical nitrogen (SCN), supercritical hydrogen (SCH), and supercritical argon (SCAR) are to be maintained at and above critical pressure (Pc) and critical temperature (Tc). This results in the development of stresses in the former material such as corrugated steel pipe (CSP) through which coolant is passed. In the present work, an investigation is performed to find mechanical behavior of CSP with different geometries of corrugations such as Circular(C-type), triangular (T-type) and rectangular(R-type). It is observed that, in the CSP with T- type corrugation experiences large stresses as compared to other corrugation geometries. Further, it is also found larger deformations in T-type corrugations lead to failure of CSP.

CONTENTS

LIST OF FIGURES

LIST OF TABLES

1 INTRODUCTION

1.1 Energy system and Background

Energy can neither be created nor be destroyed it only transforms from one state to another, the statement of 1st law of thermodynamics. At present, the growth of population is increasing day-by-day; thereby the energy consumption is also found to be increase. India is the second largest population country in the world and population growth rate is larger compared to world population growth rate. Now due to very large population growth rate, world is facing energy crisis in generation, transmission and storage sectors. Electrical energy is widely used form of energy. In order to generate energy, various methods are used like solid fuel (coal), liquid fuel (gasoline, diesel), gaseous fuel (natural gas), atomic energy, hydro-power, bio-fuels, geothermal energy, solar energy and wind energy. Out of which solar and wind are renewable energy sources and rest come under non-renewable sources. If the non-renewable sources are vanished away then it will be very difficult to generate electrical energy. In order to avoid such conditions, the amount of electrical energy that is generated should be utilized completely i.e. with no losses.

The energy that which is generated from the renewable or non-renewable sources is transmitted and distributed to the utility completely without any losses. During these transmissions the losses are occurring in the form of heat convection. In order to overcome such issues a new concept called superconductivity is introduced. The main focus of this concept is in designing the geometries of a corrugated steel pipe (SS316LN) and by passing the three cryogenic fluids such as supercritical nitrogen (SCH), supercritical hydrogen (SCH), supercritical argon (SCAR) in to the HTS cable.

Therefore, by implementing this new concept superconductivity along with the development of technology would significantly reduce the heat losses. This dissertation aimed to address some of the issues encountered in the development of geometry of HTS cable and the cryogenic fluid to be passed, mainly the mechanical properties of HTS cable.

2 TERMINOLOGY

2.1 SUPERCRITICAL FLUIDS

In 1822, Baron Charles Cagniard de La Tour discovered supercritical fluids (SCFs). A supercritical fluid is any substance at a temperature and pressure above its critical point as shown in the Figure 2-1. And at this point, distinct liquid and gas phases do not exist. These fluids consist of properties of both liquid and gases and form a new state of matter.

At the critical point, the gas-liquid interface disappears and the fluid exhibits unique transport and thermodynamic properties. These properties consists of liquid like densities which leads to significant increase in solubility, and gas-like diffusivities and viscosities and also zero surface tensions which further benefits in mass transfer and fluid mixing. The new state of fluid is highly compressible than the liquid phase thus density becomes a strong variable of both temperature and pressure which leads to adding more complexion in order to understand the flow behavior and reaction mechanism for practical models.

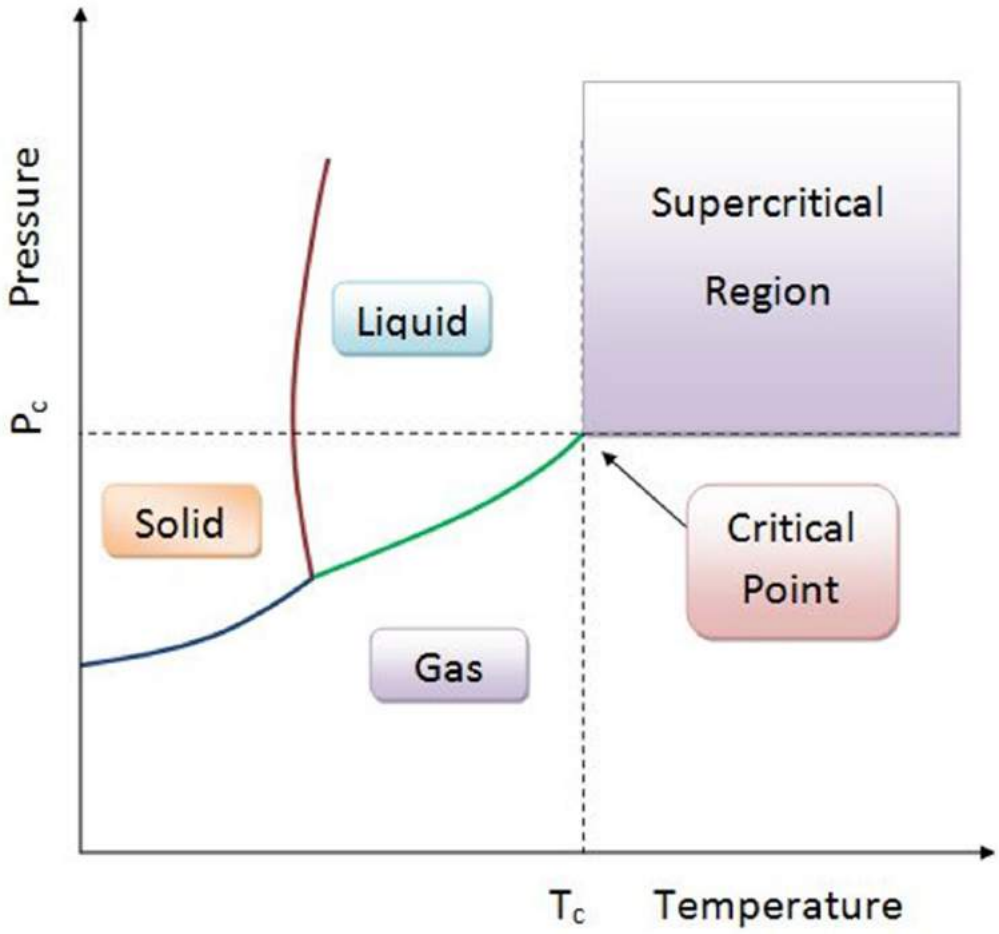

Figure 2-1 A typical P-T phase diagram of a pure substance.

2.1.1 Some facts about Supercritical Fluids

- Since the supercritical fluid have low viscosities like gases and high density like liquids, this makes it impossible to liquefy the matter using any amount of pressure.
- Close to the critical point, any small changes in pressure or temperature results in large variations in densities. Thus, by changing the temperature or pressure of the fluid, the properties can be "tuned" to be more liquid or more gas-like as per requirements.
- Solubility, at constant temperature, in a supercritical fluid tends to increase with density of fluid. Since density tends to increase with pressure which leads to increase in solubility also. Solubility tends to increase with temperature, at constant density.

2.2 Superconductivity

Superconductivity is a phenomenon of exactly zero electrical resistance and expulsion of magnetic fields occurring in certain materials when cooled below a characteristic critical temperature. It was first identified by Kamerlingh Onnes on April 8 1911. As the normal conductor does not have the zero resistance value, whereas superconductor will achieve zero resistance at a particular temperature. In mercury the first superconductor was discovered at 4K. The superconductor TlBaCaCuo was obtained at 200K.In future we can expect the superconductors will obtained at room temperature. Superconductivity is characterized by the Meissner effect, as the complete repulsion of magnetic field lines from the inner surface of the superconductor, as it transmits into the superconducting state.

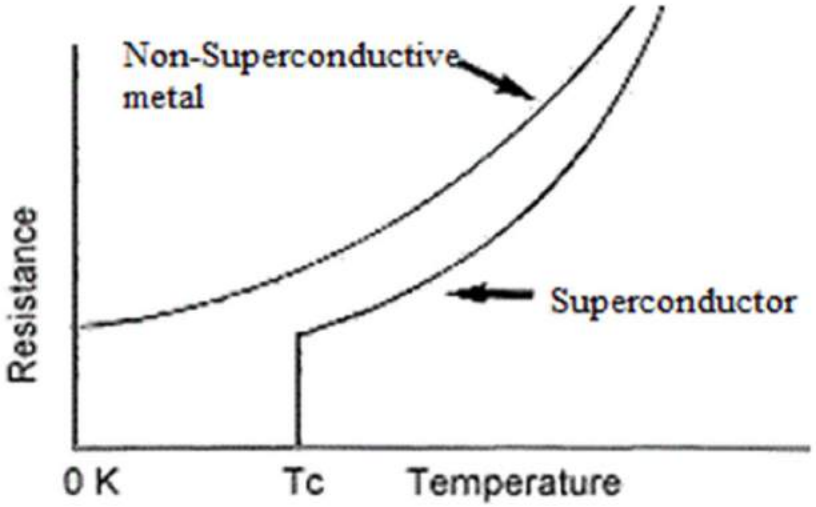

Figure 2-2 Resistance v/s Temperature Plot

2.3 Meissner effect

In the presence of an applied magnetic field, cooling the superconductor below critical temperature (T_c) is the phenomenon of Meissner effect as shown in Figure 2-3. Below the critical temperature the samples cancelled nearly all interior magnetic fields. They will identify this effect only indirectly because of the magnetic flux is conserved by a superconductor, when the interior lines field decreases, the exterior field increases[1]. The phenomenon of losing its resistivity when sufficiently cooled to a very low temperature (below a certain temperature). This temperature is known as Critical temperature (T_c).

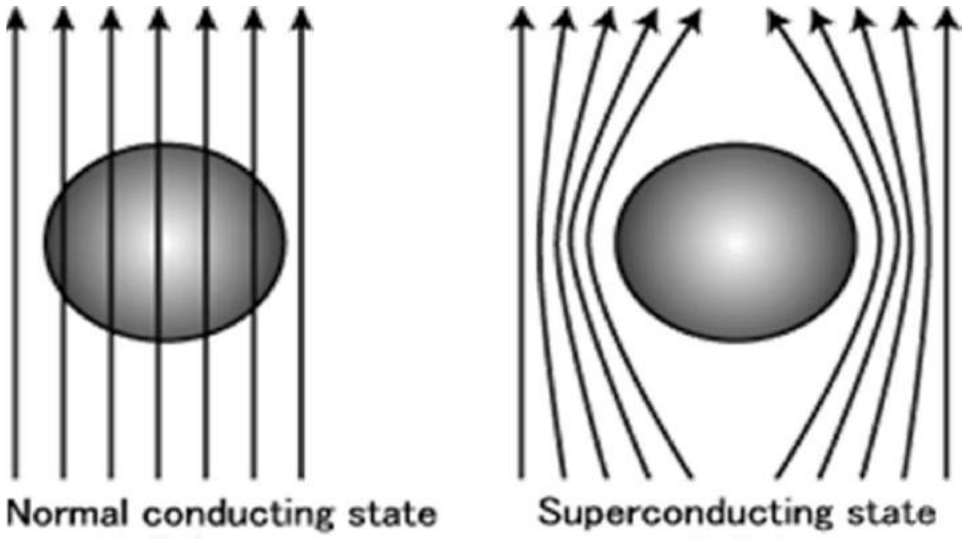

Figure 2-3 Meissner effect

2.4 Superconductors

In an ordinary electrical conductor the incoherent disorder electrons allow penetration by an external magnetic field, whereas in superconductor the coherent collective function of electrons spontaneously exclude an external magnetic field and maintain its penetrable status.

The Meissner effect differentiates a superconductor and a perfect electrical conductor. In the presence of an applied magnetic field (H) two types of superconductors are formed. These are generally referred as Type-I and Type-II .When the superconducting material is placed in a magnetic field under the condition when $T \leq T_C$ and $H \leq H_C$, the flux lines are excluded from the material. Superconductors are developed for power engineering applications like transformers, power transmission cables, fault current limiters (FCL) motors and generators.

2.4.1 Types of superconductors

There are mainly two types of superconductors. They are as follows:

- **Type-1 superconductors**

The identifying characteristics are zero electrical resistivity below a critical temperature, zero internal magnetic fields (Meissner effect) and a critical magnetic field above which superconductivity ceases. The best superconductors at room temperature (gold, silver and copper) do not become superconducting at all. These have limited practical usefulness because the critical magnetic fields are very small and the superconducting state disappears suddenly at that temperature. Examples are uranium, lead, aluminium, beryllium etc.

- **Type-2 superconductors**

Superconductors made from alloys are called as Type-2 superconductors. These are mechanically hardening than Type-1.They exhibit much higher critical magnetic field. These are usually exit in mixed state of normal and superconducting regions. Examples are NbN, NbTi, and PbMoS etc.

2.4.2 Critical temperatures for superconductors

It is defined as temperature at which the electrical resistivity of a metal drops to zero. As the differences are occurring a separation is made on the basis of attainability of T_c of superconducting compounds into two groups. They are High Temperature superconductors (HTS) at a T_c of 40K and Low temperature superconductors (LTS) having a record of T_c of 23K.

2.5 Cryogenic fluids

It is defined as studying the behavior of materials at low temperatures. However at low temperature they are in liquid form. Even the gases and vapors that are coming out are very cold. Different cryogens will become into liquids at different temperatures and pressures. Hence these fluids are very flammable. When passing a high amount of electricity through these HTS cables heat is produced inside it so in order to cool these cryogenic fluids are used.

Table 2-1 Critical Points for different cryogenic coolants[2]

Types of Cryogenic Coolant	Critical Temperature (Tc)	Critical Pressure(Pc)
SCH	33.190K	13.15 bar
SCN	126.19K	33.958 bar
SCO	154.58K	50.43 bar
SCAR	150.69K	48.63 bar

2.6 HTS Cable

As mentioned above that the losses occurring in power transmissions, these HTS cables (Figure 2-4) are used to overcome. Superconducting High Power Transmission Cable transmits 5 to 10 times the electrical current of traditional copper or aluminum cables with significantly improved efficiency when compared to normal conductor. Various components of HTS cable are:

- Former
- HTS tapes
- Thermal insulation
- Dielectric material
- Cryostat etc.

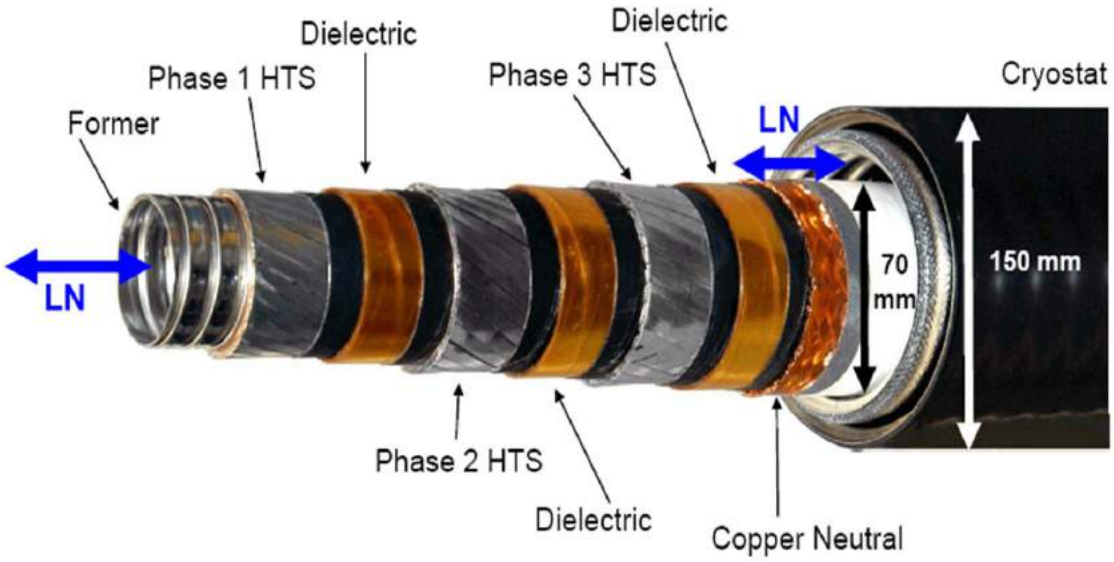

Figure 2-4 Standard HTS cable [2]

These cables are used to transmit power for a long distances during this the change in the path direction is occurred in such a cases the cable should be bend during this bending the former that which is present inside should have the corrugations. When the superconductor cable carries the alternate current, the AC losses will be produced. While carrying direct current, there is nearly no losses produced. Therefore, compare with the HTS AC power cable, HTS DC power cable has more transmission efficiency. In future high-current long-distance DC HTS power cable will play an important role in power transmission systems.

2.6.1 Stainless steel (SS316LN)

Stainless steel grade 316LN is an austenitic type of steel that it is a low carbon, and is of grade 316 steel. Some amount of Nitrogen is present in this where the content of steel provides solid solution hardening, and raises its minimum value of yield strength. It also has good resistance for its general corrosion or pitting corrosion.

2.6.2 Properties of Stainless steel

The advantages of using SS316LN material is as follows.

- Material cost savings
- Corrosion protection
- Ease of fabrication
- Long pipe lengths
- Erosion resistance

Table 2-2 Properties of SS316LN[2]

Properties	Metric
Tensile strength	515Mpa
Yield strength	205Mpa
Modulus of elasticity	190-210Mpa
Poisons ratio	0.27-0.30

2.6.3 Advantages of HTS cables

- Current carrying capability is 3-5 times better than a normal conductor
- No electrical losses
- Lesser in space
- High capacity inter connects

2.6.4 Applications of HTS cables

- Current leads
- Induction heater magnets
- Motors
- Extraction of oil seeds
- Aircrafts
- Marine ships
- Magnetic Resonance Imaging(MRI)

2.6.5 Mechanical properties

In order to investigate the feasibility of a former to be used in HTS cable at different critical pressures of cryogenic fluids with different corrugations, various properties are to be investigated. They are as follows:

- Total deformation
- Directional deformation
- Equivalence stress
- Maximum principal stress
- Maximum shear stress
- Equivalent elastic strain
- Maximum principal elastic strain
- Maximum shear elastic strain
- Shear elastic strain
- Strain energy

Moreover, in this analysis the temperature dependent properties of stainless steel (SS316LN) were not considered. Only the pressure variations are given corrugations and with respect to the cryogenic fluids.

3 REVIEW OF LITERATURE

T. Nakatsuka et al., (2014)[1]**:** Research and develop the basic technology of HTS cable, fault current limiter, and transformer. Also study the 3 kA superconducting cable, cooling technology of HTS cable length 500m and power system analysis of cable and AC equipment's. The basic technologies have been started for the design of HTS cable by testing works. The feasibility studies for HTS cable also have been studied by power system analysis.

RajaSekhar Dondapati et al., (2013)[2]**:** Thermo physical properties of LN2are considered to be temperature dependent. Pressure drop and heat transfer carried out for different flow rates of LN2.At constant corrugation depth, the pressure drop increases with increases in corrugation pitch. In order to increase heat transfer twisted tapes are inserted by creating turbulence.

Dong Zhang et al., (2012)[3]**:** 5 m/10 kA HTS DC power cable was developed which helps to investigate the design of a conductor, fabrication, current carrying capacity and stability of the 360 m/10 kA HTS power cable. A 5 m/10 kA HTS DC power cable has been designed, fabricated and tested to evaluate the performance of the 360 m/10 kA HTS DC power cable, which connect the rectifier output of a substation with the bus bar of an electrolytic aluminium cell in Henan Zhongfu Industrial.

Francesco Grilli et al., (2012)[4]**:** Evaluated the ac losses of HTS tapes and wires as well as of assemblies such as cables and coils. The formulation, used in the magnetic field components as state variables, had proved an efficient implementation to solve 2-D problems, which involves infinitely long or axially-symmetric geometries. A 3-D model for time-dependent Simulations of high-temperature superconductors using the H-formulation is successfully implemented. The model has been validated by comparing the results with cases that can be solved in 2-D and has been used to show different examples of application on 3-D geometries.

Marijn Oomen et al., (2012)[5]**:** Investigate the use of 2nd-generation High-Temperature Superconductors (2G-HTSs) in the rotors of electrical motors and generators. It is operated in vacuum at temperatures around 30 K, in strong magnetic fields of about 2T.Impregnated Coils are desirable. Several of the coils show degradation of the superconducting properties. Three large impregnated 2G-HTS racetrack coils with kA current capacity were produced and successfully tested. Mechanical properties of 2G-HTS, their uniformity and fatigue behavior are studied.

Schmidt et al.,(2009)[6]**:** The integration of a high voltage cable in a networks always a particular case and in field of superconducting cables several designs are already available to fulfill the technical and environmental requirements. Superconducting cables have significant benefits for power transmission and distribution applications that provide new aspects and possibilities in network planning and operation.

S.C. Kim et al., (2007)[7]**:** Two different Ag round wires are considered with different Ag ratio were fabricated by using powder in tube method and processing factor at each step was investigated. Microstructure after pre-annealing was investigated. Drawing stresses of two wires at first and second bundle wire are almost the same. In order to evaluate the uniformity of filaments, investigated COV of the wires. Higher Ag ratio wire shows better COV characteristic, suggesting that higher Ag ratio wire has better filament uniformity.

Tosin Famakinwa et al., (2007)[8]**:** The eddy current losses in the matrix of two twisted filaments Bi-2223 HTS tapes in applied external AC magnetic field was calculated using 3D FEM software. Numerical calculation results shows that the Contribution of eddy current loss at commercial frequency is not minimum. The numerical results presented are for uncoupled filaments HTS tapes.

T. Hemmia et al., (2006)[9]**:** Study the current decay behaviors in HTS coils using Bi-2223/Ag tapes. Demonstrate that the resistance is enhanced due to the decay of the shielding current by the flux creep and flux flow. Results are compared with numerical analysis using a FEM. Current decay behavior is also discussed by choosing an overshooting excitation technique. The current decay behaviors are found to be affected by shielding currents. Improvement in decay behaviors is possible using appropriate excitation process like overshooting the initial current. It is determined by the joint resistance.

H.J.Kim et al., (2004)[10]**:** This paper is based on the study of electrical insulation properties of dielectric paper, such as breakdown voltage, partial discharge, which is one of the HTS cable structure elements. The PPLP had a high tensile stress in liquid nitrogen, but low tensile strain. As tensile stress increased the breakdown stress of PPLP was decreased because of micro crack occurrence.

Mitsuho Furuse et al., (2003)[11]**:** Establishment of long distance cooling techniques and design of a compact cross section are required for development of HTS cables. Temperature distributions of counter flow cooled HTS power cable and designed 3 different cable structures. These are effective from the view point of cooling design to produce compact cables**.**

Chikashi Suzuki et al., (2003)[12]**:** In this paper an investigation is done on the optimal design for the cabling parameters, Cross sections of pitch length, dimensions of tape for YBCO and former diameter. Transverse bending strain can be calculated with the cabling parameters longitudinal bending strain can also be calculated.

Takato Masuda et al., (2002)[13-20]**:** Developed a 3-core 66 kV class HTSC cable and shield wound with Ag–Mn sheathed Bi-2223 tapes, insulation with polypropylene laminated paper impregnated with liquid nitrogen and thermal insulation with Co-axial corrugated pipes. The results of these tests clarifies good performance of the cable such as critical current value 2.4 kA, AC loss with 0.5 W/m/phase at 1 kA and AC 130 kV withstand voltage. Cable has the basic electric properties required to a 66 kV HTSC cable.

4 SCOPE OF THE STUDY

We know that, High Temperature superconductors (HTS) play a vital role in superconducting Power grid. HTS cables are cooled by various cryogenic coolants (fluids) in order to remove the infiltrated or deposited heat loads. So, the dispersion of HTS cables in power transmission and distribution may lead to improve the performance of power grid.

The study will undergo the analytical work which is based on analyzing the temperature dependent properties and mechanical properties of HTS cables.

By passing different types of cryogenic fluids

The study will check the heat transfer, stress formations, capability of a former and the different cryogenic fluids. However, the fluids are passed into the HTS cable to cool and again the same analysis will be performed. Then the comparison will be done among the cryogenic fluids.

From the mechanical properties of stainless steel pipe the stresses at which they are occurring and the numerical analysis is to be done between the minimum and maximum stresses. Finally the geometry of the corrugated steel pipe having less stresses is chosen with respect to the cryogenic fluid to be cooled. The power is transmitted through under the ground of earth's surface by HTS cables and heat losses are reduced. Moreover high efficiency of power generated is achieved.

5 OBJECTIVES OF THE STUDY

- ✓ To enhance the mechanical properties of a corrugated steel pipe of HTS cable by passing the different cryogenic fluids such as:
  - ❖ Total deformation
  - ❖ Directional deformation
  - ❖ Equivalence stress
  - ❖ Maximum principal stress
  - ❖ Maximum shear stress
  - ❖ Equivalent elastic strain
  - ❖ Maximum principal elastic strain
  - ❖ Maximum shear elastic strain
  - ❖ Strain energy
  - ❖ Shear elastic strain

- ✓ To compare the mechanical properties of stainless steel former at different corrugations by passing different cryogenic fluids.
- ✓ To enhance the efficiency of power transmission and stresses that is obtained in HTS cable.
- ✓ To study the mechanical properties and stresses those are obtained.
- ✓ Obtaining the high power efficiency by reducing the heat losses.

6 RESEARCH METHODOLOGY

- The analysis will be required three types of corrugations geometries. These are C-type, T-type, R-type and giving the critical pressures and temperatures that which are taken from the NIST-REFPROP software.

- Considering the mechanical properties of all the three geometries the stresses obtained will be observed.

- The geometry of a corrugated steel pipe (SS316LN) is considered in ANSYS14.5 version with one Cross sections and the dimensions are Diameter= 20mm, Length= 21mm, Thickness= 1mm, Corrugation depth= 1mm respectively for the three corrugations. After drawing the geometries it is meshed to point 0.0005mm and the loads as x, y, z components are fixed as constants. Applying the pressures inside the pipe in all directions from the critical pressures of SCH, SCAR, SCN respectively and by increasing 1 bar from P_c eight pressures are considered for each cryogenic fluid. Obtaining the maximum and minimum values of the ten mechanical properties and drawing statistical graphs are drawn. After analyzing all the stresses concluding the corrugation is having minimum stresses and which gases are more suitable is identified.

Table 6-1 critical temperature and critical pressure

Cryogenic Fluid	Critical Temperature	Critical Pressure
Super Critical Nitrogen	126.19K-132.19K	33.958bar – 40.958bar
Super Critical Hydrogen	33.190K- 40.190K	13.150bar – 20.150bar
Super Critical Argon	150.69K-158.69K	48.63bar – 55.63bar

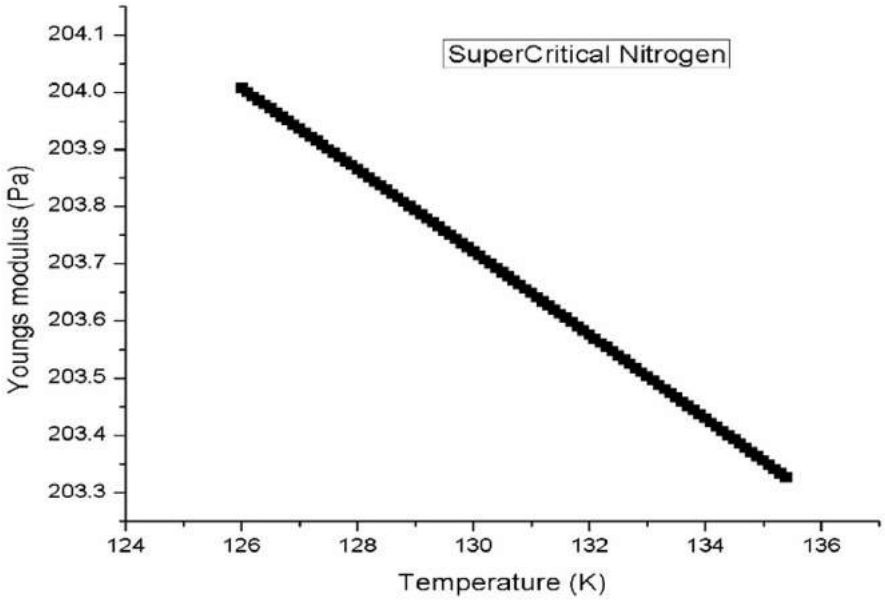

Figure 6-1 Temperature (SCN) vs Young's modulus

The Figure 6-1 shows the variation of young's modulus of corrugated steel pipe in the operating temperature range (126.19K to 132.19K) of supercritical nitrogen. It is observed that a linear variation of young's modulus contributes to linear stresses developed in the corrugated steel pipe while operated with SCN. This can also be confirmed from Figure 6-2.

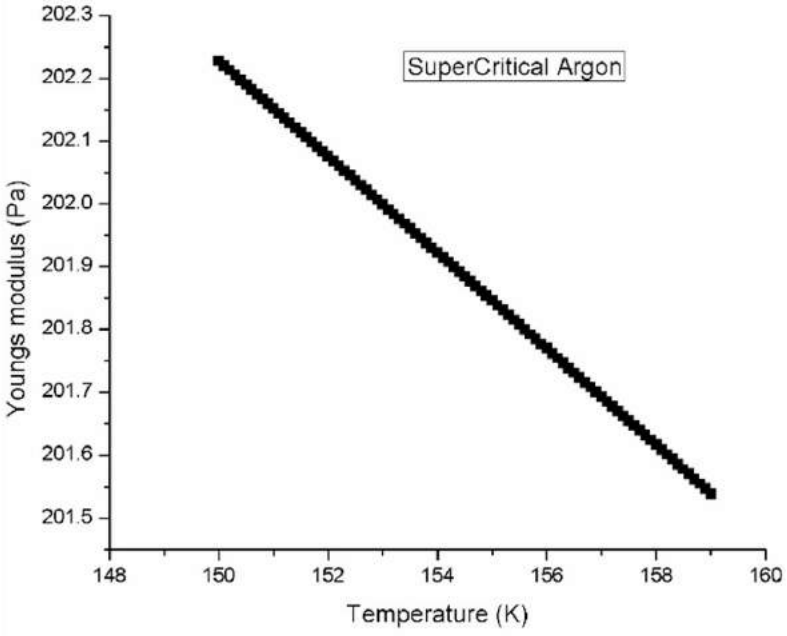

Figure 6-2 Temperature (SCAR) vs. Young's modulus

The above figure shows the variation of young's modulus of corrugated steel pipe in the operating temperature range (150.69K to 158.69K) of supercritical argon. It is observed that a linear variation of young's modulus contributes to linear stresses developed in the corrugated steel pipe while operated with SCN. This can also be confirmed from figure 6.1.2.

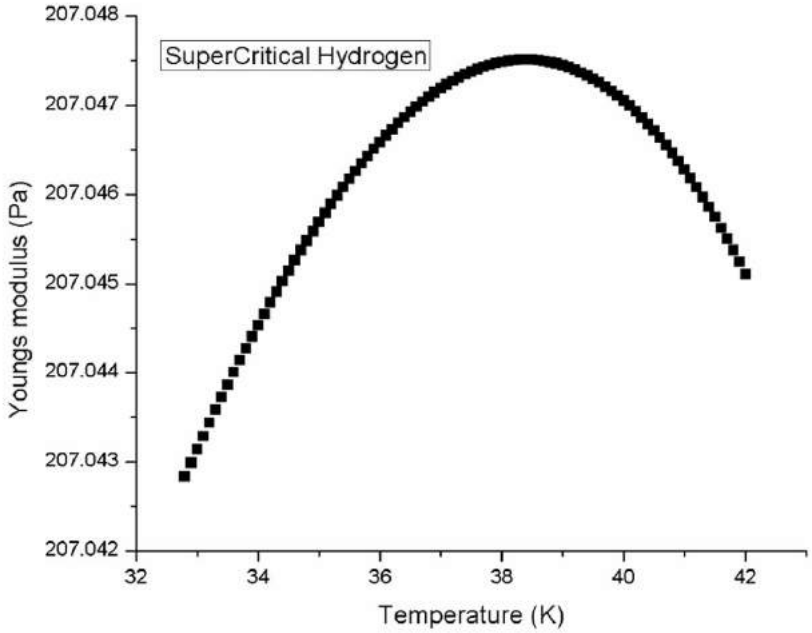

Figure 6-3 Temperature (SCH) vs. young's modulus

The above figure shows the variation of young's modulus of corrugated steel pipe in the operating temperature range (33.19K to 40.19K) of supercritical hydrogen. A non-linear variation in young's modulus with respect to temperature is observed that which contributes to non- linear stresses accumulated in various types of corrugations geometries as seen in Figure 6-3.

7 RESULTS AND DISCUSSION

7.1 Without Temperature dependent properties

Applying the pressures internally by fixing the three coordinates and without giving the temperature dependent properties respectively to observe the stresses that are obtained.

7.1.1 Variation of Directional Deformation

From the Figure 7-1, it can be observed that directional deformation is plotted against the applied pressures. It can also be observed that maximum directional deformation is experienced in corrugated steel pipe having circular corrugation. This may be due to the low young's modulus value and stresses occurred in circular corrugations. Similarly, the lowest directional deformation is found in corrugated steel pipe having triangular corrugations. Moreover, if the pressure increases the directional deformation also increases. The location of the maximum and minimum deformation is shown in Figure 7-2.

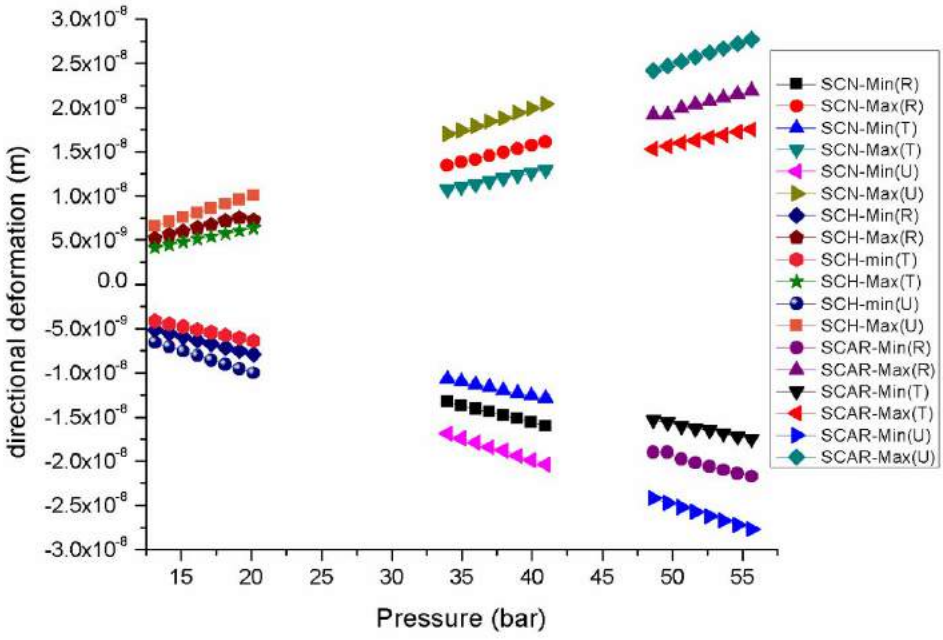

Figure 7-1: Directional deformation with respect to pressure

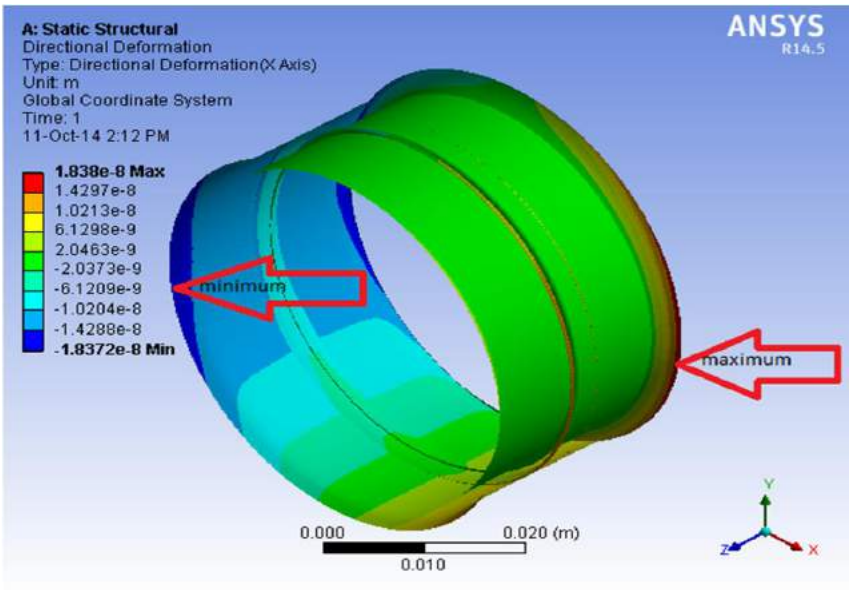

Figure 7-2: Directional deformation rectangular cross section

7.1.2 Equivalent Stress

From the Figure 7-3, it can be observed that equivalent stresses are plotted against the applied pressures. It can also be observed that maximum equivalent stresses are experienced in corrugated steel pipe having triangular corrugation. This may be due to the low young's modulus value and having sharp edges, stresses occurred in triangular corrugations. Similarly, the lowest equivalent stress is found in corrugated steel pipe having rectangular corrugations. Moreover, if the pressure increases equivalent stress also increases. The location of the maximum and minimum stresses is shown in Figure 7-4.

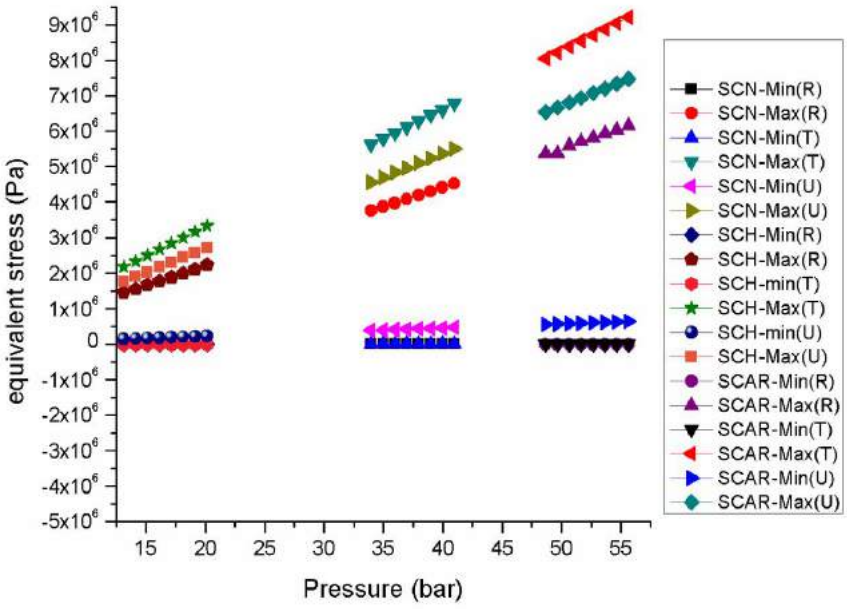

Figure 7-3: Equivalent stress with respect to pressure

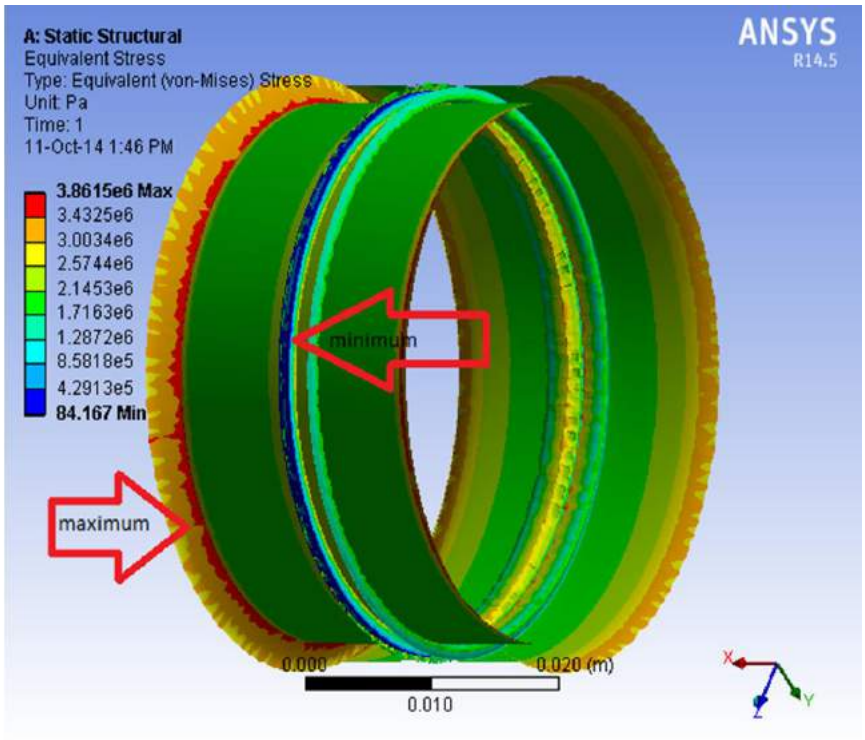

Figure 7-4: Equivalent stress rectangular cross section

7.1.3 Variation of Maximum Principal Stress

From the Figure 7-5, it can be observed that maximum principal stresses are plotted against the applied pressures. It can also be observed that maximum principal stresses are experienced in corrugated steel pipe having triangular corrugation. This may be due to the low young's modulus value and having sharp edges, stresses occurred in triangular corrugations. Similarly, the lowest maximum principal stress is found in corrugated steel pipe having circular corrugations. Moreover, if the pressure increases maximum principal stress also increases. The location of the maximum and minimum principle stresses is shown in Figure 7-6.

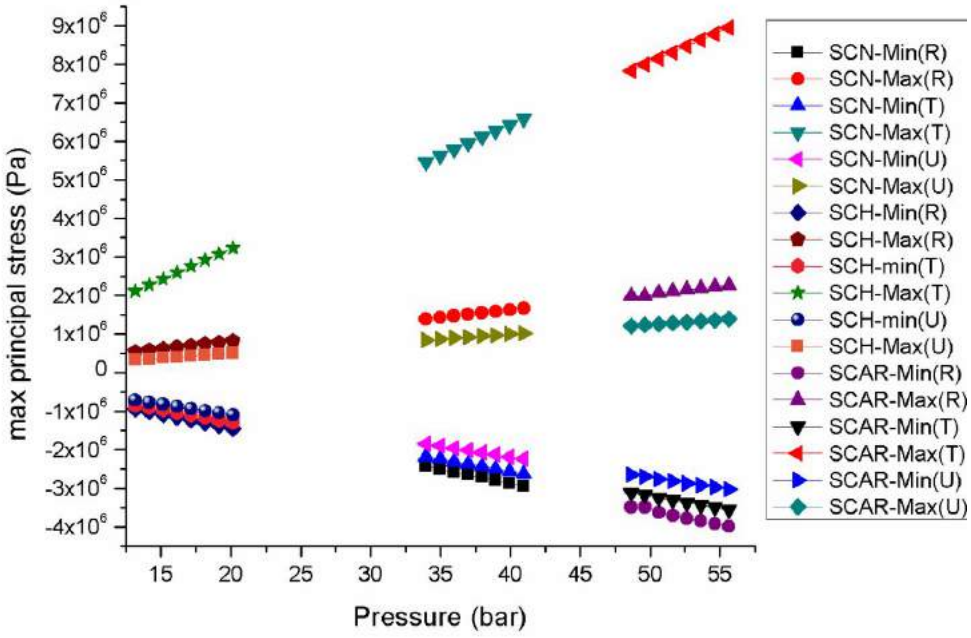

Figure 7-5 Maximum principle stress with respect to pressure

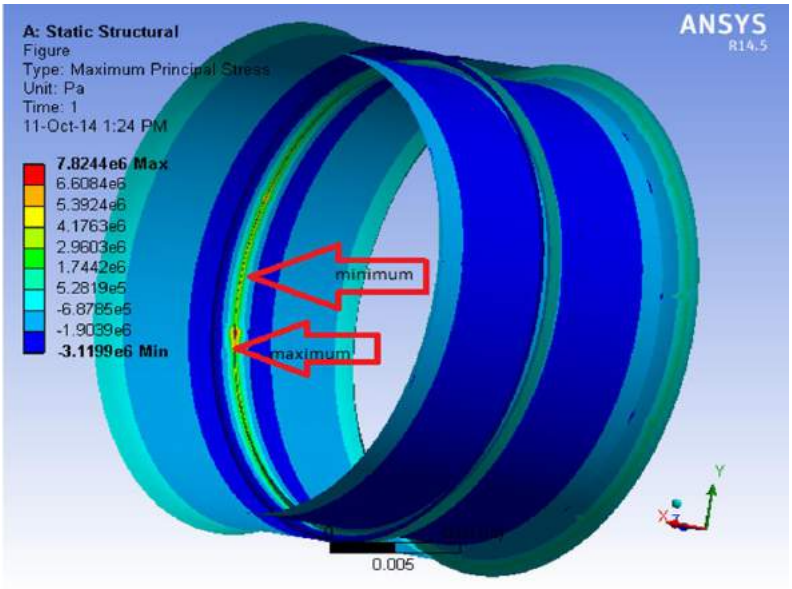

Figure 7-6: Maximum principle stress rectangular cross section

7.1.4 Variation of Equivalent Elastic Strain

From the Figure 7-7 , it can be observed that equivalent elastic strain are plotted against the applied pressures. It can also be observed that maximum equivalent elastic strain are experienced in corrugated steel pipe having triangular corrugation. This may be due to the low young's modulus value and having sharp edges, stresses occurred in triangular corrugations. Similarly, the lowest equivalent elastic strain is found in corrugated steel pipe having rectangular corrugations. Moreover, if the pressure increases equivalent elastic strain also increases. The location of the maximum and minimum deformation is shown in Figure 7-8.

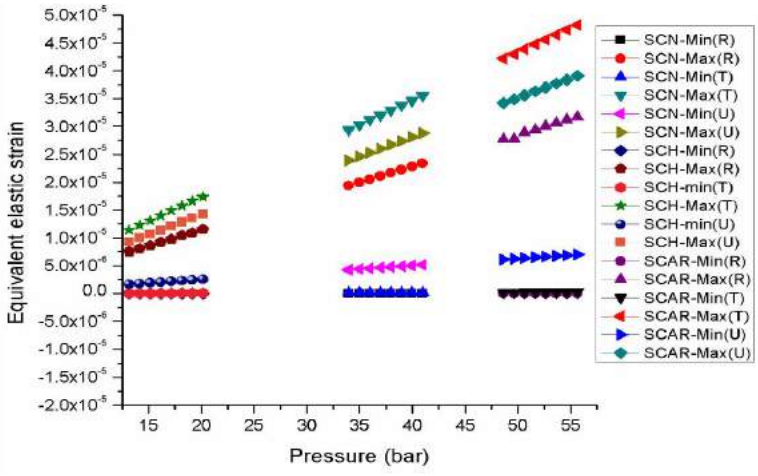

Figure 7-7: Equivalent elastic strain with respect to pressure

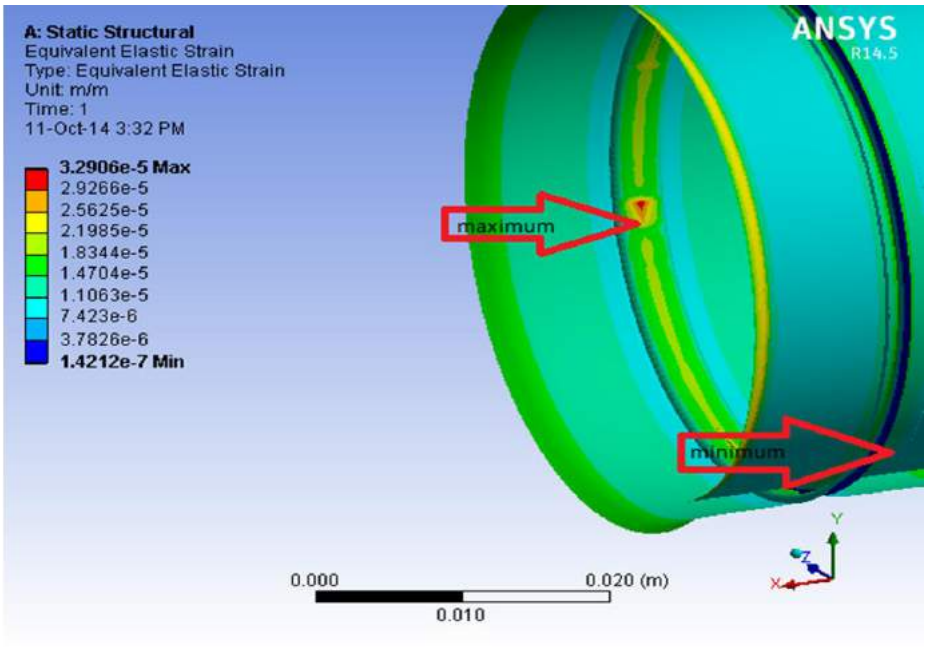

Figure 7-8: Equivalent elastic strain circular cross section

7.1.5 Variation of Maximum Principal Elastic Strain

From the Figure 7-9, it can be observed that maximum principal elastic strain are plotted against the applied pressures. It can also be observed that maximum principal elastic strain are experienced in corrugated steel pipe having triangular corrugation. This may be due to the low young's modulus value and having sharp edges, stresses occurred in triangular corrugations. Similarly, the lowest maximum principal elastic strain is found in corrugated steel pipe having rectangular corrugations. Moreover, if the pressure increases maximum principal elastic strain also increases. The location of the maximum and minimum deformation is shown in Figure 7-10.

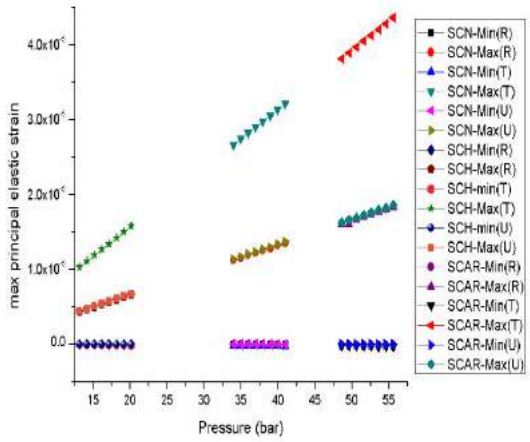

Figure 7-9: Maximum principal elastic strain with respect to pressure

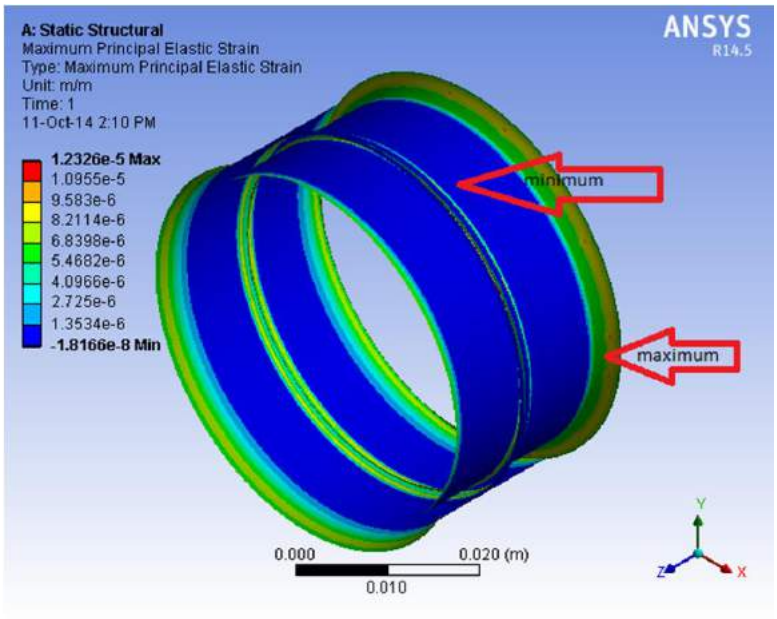

Figure 7-10: Maximum principal elastic strain rectangular cross section

7.1.6 Variation of Shear Elastic Strain

From the Figure 7-11, it can be observed that shear elastic strain are plotted against the applied pressures. It can also be observed that maximum shear elastic strain is experienced in corrugated steel pipe having triangular corrugation. This may be due to the low young's modulus value and having sharp edges, stresses occurred in triangular corrugations. Similarly, the lowest shear elastic strain is found in corrugated steel pipe having circular

corrugations. Moreover, if the pressure increases shear elastic strain also increases. The location of the maximum and minimum deformation is shown in Figure 7-12.

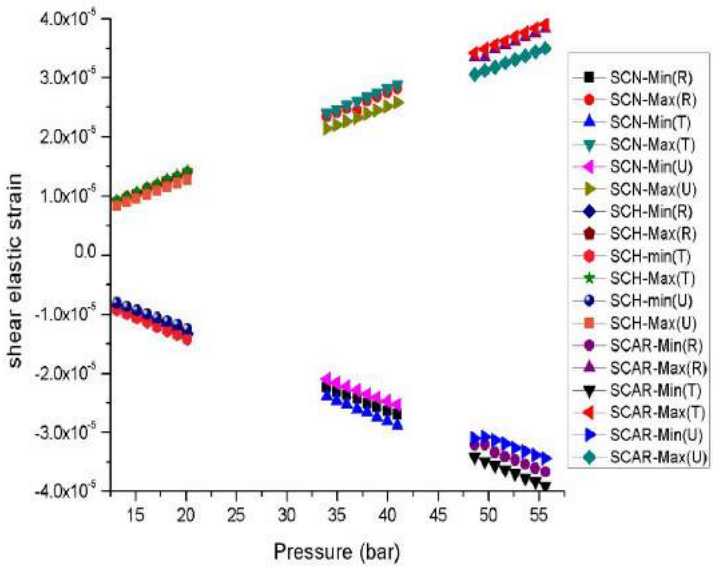

Figure 7-11: Shear elastic strain with respect to pressure

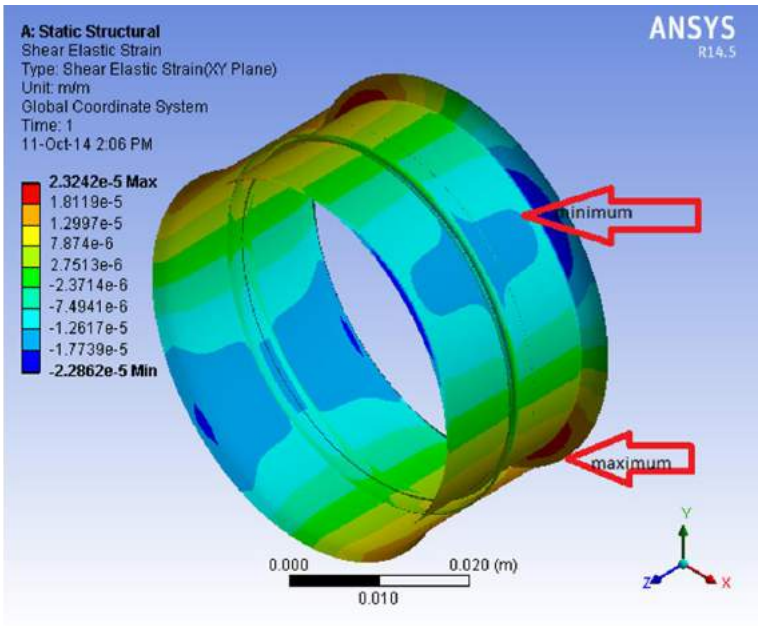

Figure 7-12: Shear elastic strain circular cross section

7.1.7 Variation of maximum Shear Elastic Strain

From the

Figure 7-13, it can be observed that maximum shear elastic strain are plotted against the applied pressures. It can also be observed that maximum shear elastic strain is experienced in corrugated steel pipe having triangular corrugation. This may be due to the low young's

modulus value and having sharp edges, stresses occurred in triangular corrugations. Similarly, the lowest shear elastic strain is found in corrugated steel pipe having circular corrugations. Moreover, if the pressure increases maximum shear elastic strain also increases in triangular corrugated pipe. The location of the maximum and minimum deformation is shown in Figure 7-14.

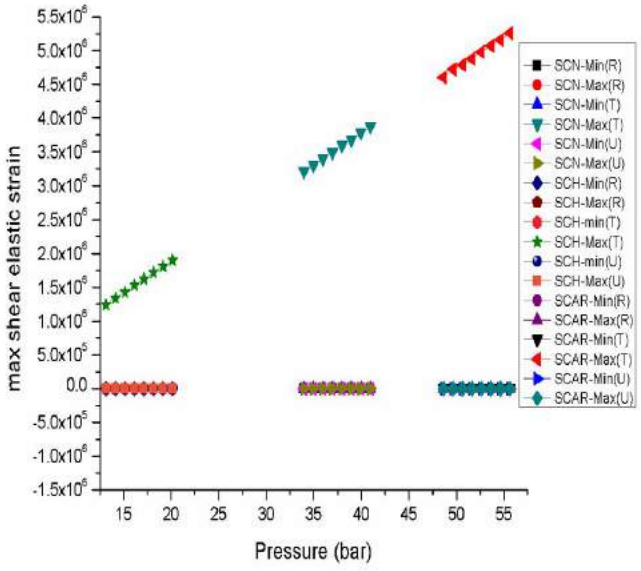

Figure 7-13: Maximum shear elastic strain with respect to pressure

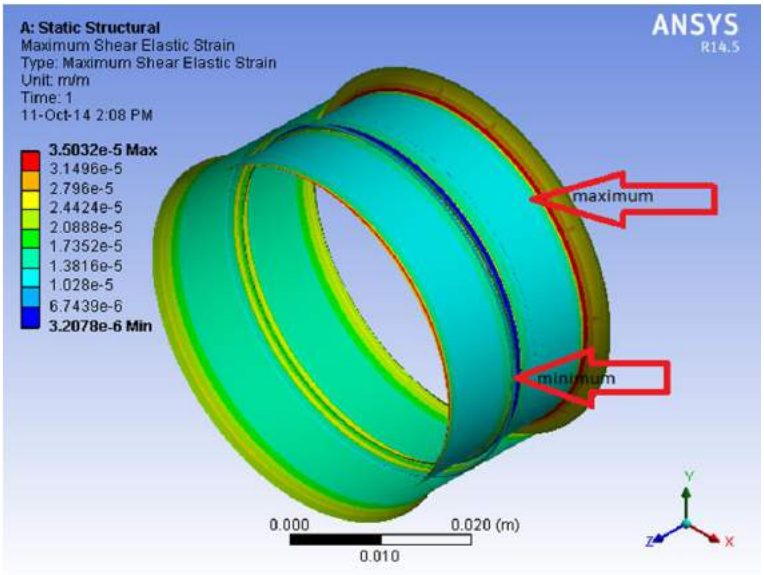

Figure 7-14: Maximum shear elastic strain circular cross section

7.1.8 Variation of Maximum Shear Stress

From the Figure 7-15 , it can be observed that maximum shear stress is plotted against the applied pressures. It can also be observed that maximum shear stresses are experienced in corrugated steel pipe having triangular corrugation. This may be due to the low young's modulus value and having sharp edges, stresses occurred in triangular corrugations. Similarly, the lowest maximum shear stress is found in corrugated steel pipe having rectangular corrugations. Moreover, if the pressure increases maximum shear stress also increases. The location of the maximum and minimum deformation is shown in Figure 7-8.

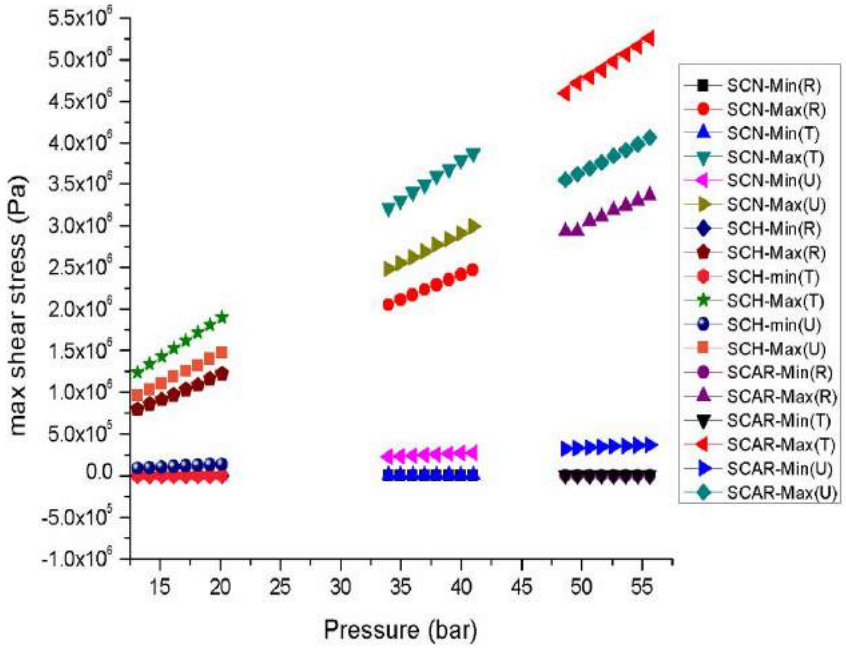

Figure 7-15: Maximum shear stress with respect to pressure

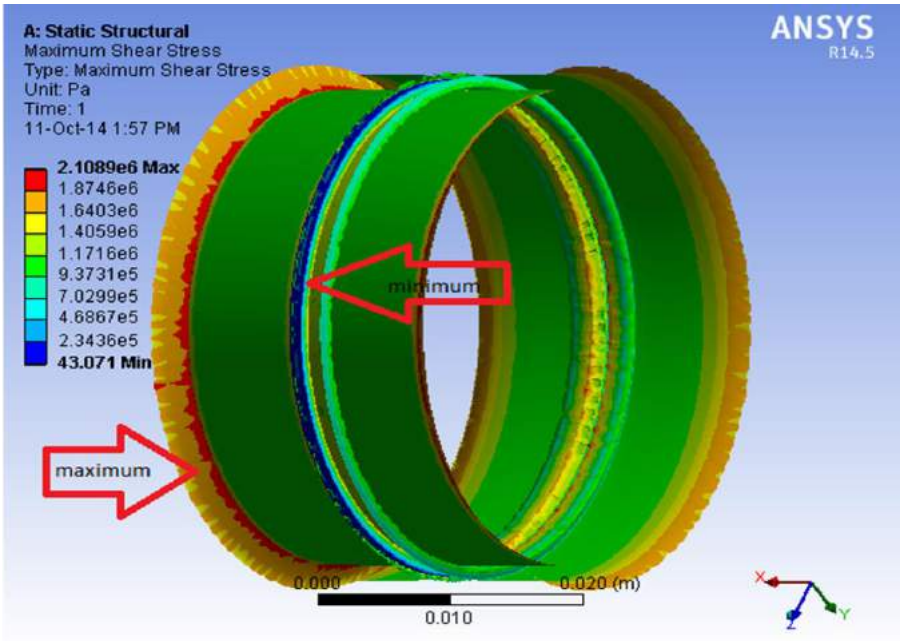

Figure 7-16 Maximum shear stress circular cross section

7.1.9 Variation of Strain Energy

From the Figure 7-17 , it can be observed that strain energy is plotted against the applied pressures. It can also be observed that maximum strain energy is experienced in corrugated steel pipe having triangular corrugation. This may be due to the low young's modulus value and having sharp edges, stresses occurred in triangular corrugations. Similarly, the lowest strain energy is found in corrugated steel pipe having circular corrugations. Moreover, if the pressure increases strain energy also increases. The location of the maximum and minimum deformation is shown in Figure 7-18.

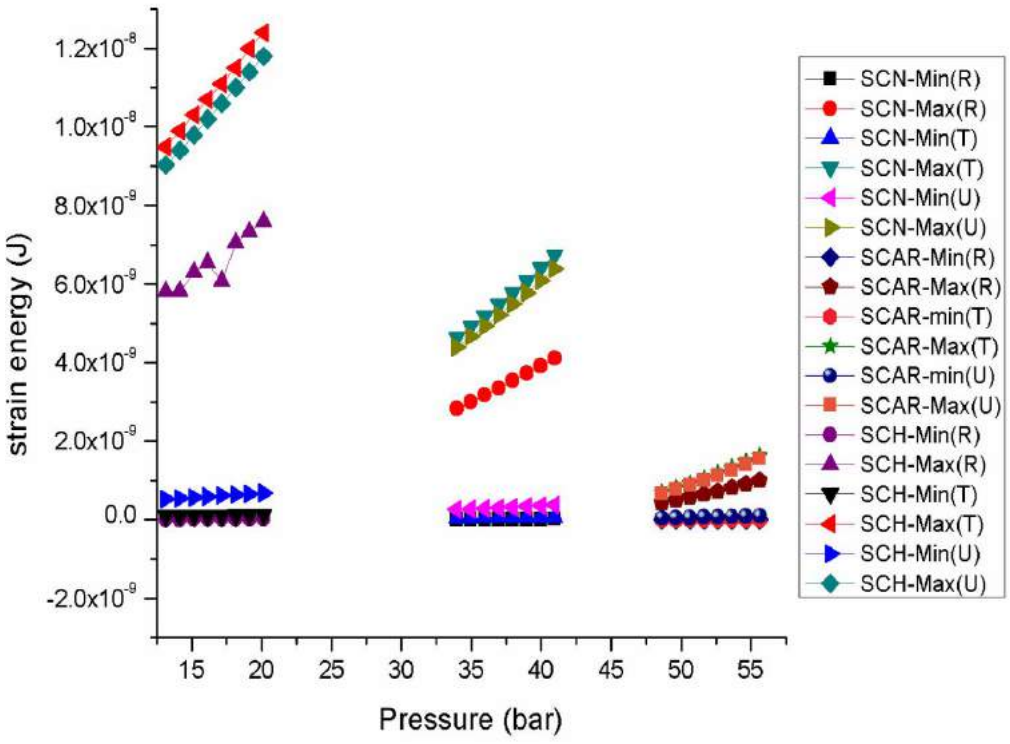

Figure 7-17 Strain energy with respect to pressure

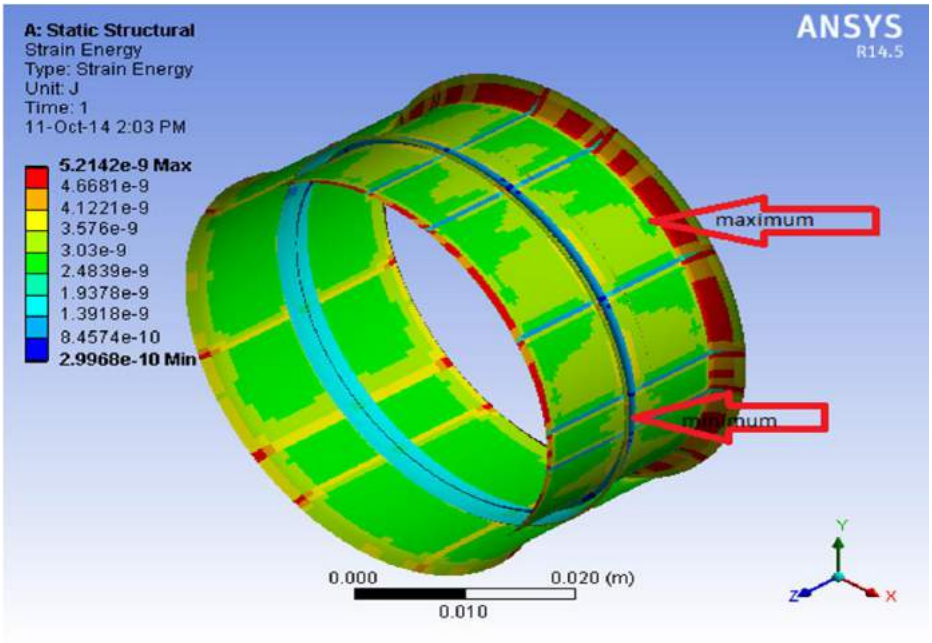

b)

Figure 7-18 strain energy circular cross section

7.1.10 Variation of Total Deformation

From the Figure 7-31, it can be observed that total deformation is plotted against the applied pressures. It can also be observed that maximum total deformation is experienced in corrugated steel pipe having triangular corrugation. This may be due to the low young's modulus value and having sharp edges, stresses occurred in triangular corrugations. Similarly, the lowest strain energy is found in corrugated steel pipe having circular corrugations. Moreover, if the pressure increases total deformation also increases. The location of the maximum and minimum deformation is shown in Figure 7-31.

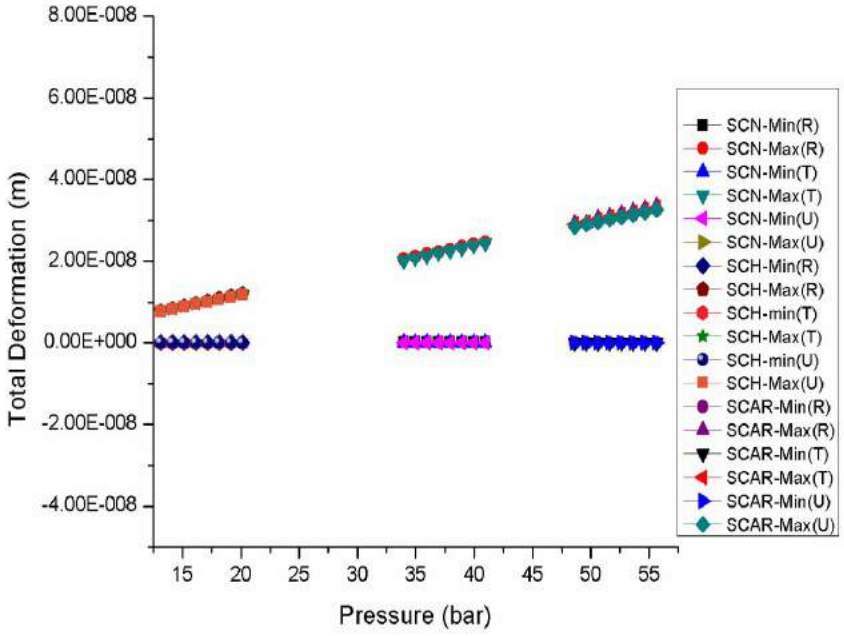

Figure 7-19 total deformation with respect to pressure

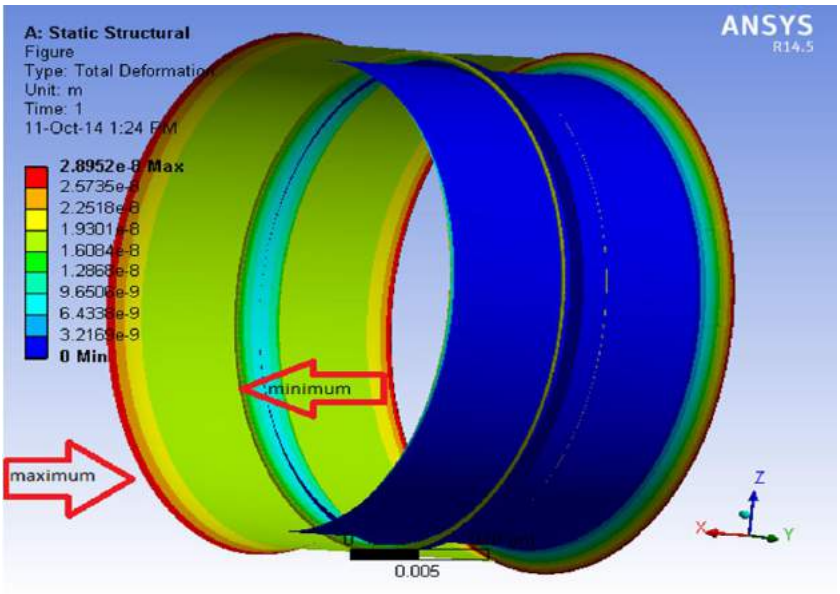

Figure 7-20 total deformation circular cross section

7.2 Temperature Dependent properties

7.2.1 Variation of Directional Deformation

From the Figure 7-22, it can be observed that directional deformation is plotted against the applied pressures. It can also be observed that maximum directional deformation is experienced in corrugated steel pipe having circular corrugation. This may be due to the low young's modulus value and stresses occurred in circular corrugations. Similarly, the lowest directional deformation is found in corrugated steel pipe having triangular corrugations. Moreover, if the pressure increases the directional deformation also increases. The location of the maximum and minimum deformation is shown in Figure 7-21.

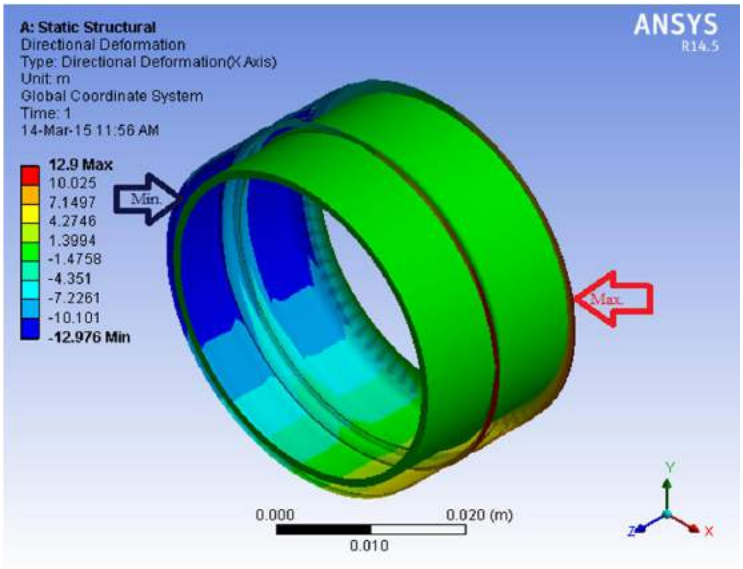

Figure 7-21 Directional deformation with respect to pressure

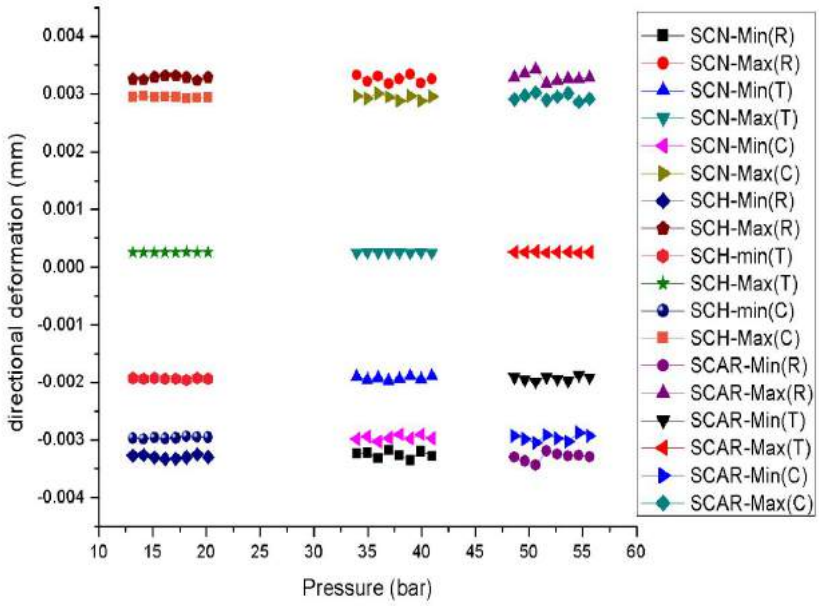

Figure 7-22 Directional deformation rectangular cross section

7.2.2 Equivalent Stress

From the Figure 7-23 , it can be observed that equivalent stresses are plotted against the applied pressures. It can also be observed that maximum equivalent stresses are experienced in corrugated steel pipe having triangular corrugation. This may be due to the low young's modulus value and having sharp edges, stresses occurred in triangular corrugations. Similarly, the lowest equivalent stress is found in corrugated steel pipe having rectangular corrugations. Moreover, if the pressure increases equivalent stress also increases. The location of the maximum and minimum deformation is shown in Figure 7-24.

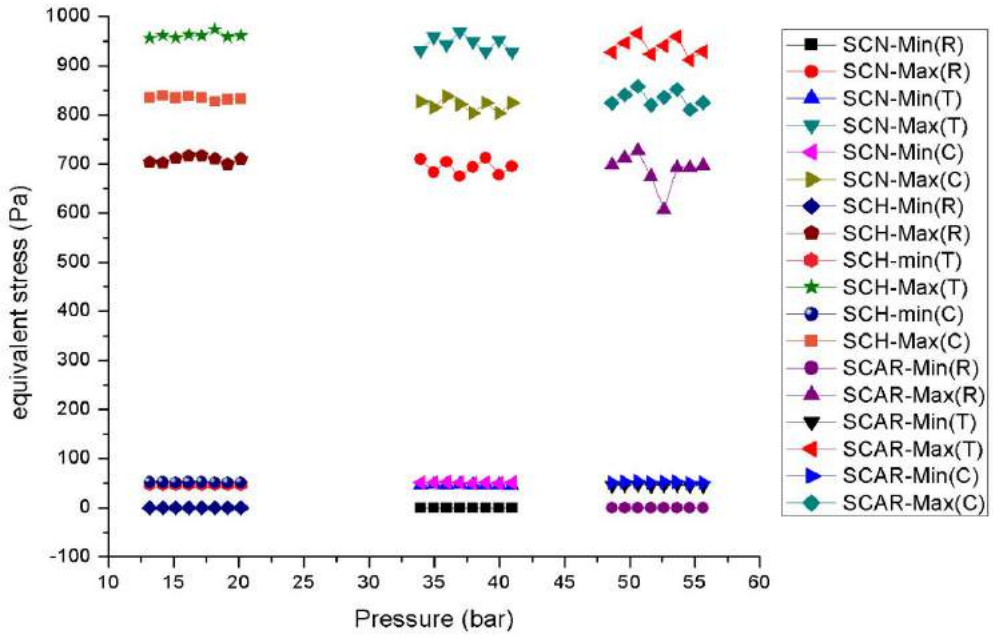

Figure 7-23 Equivalent stress with respect to pressure

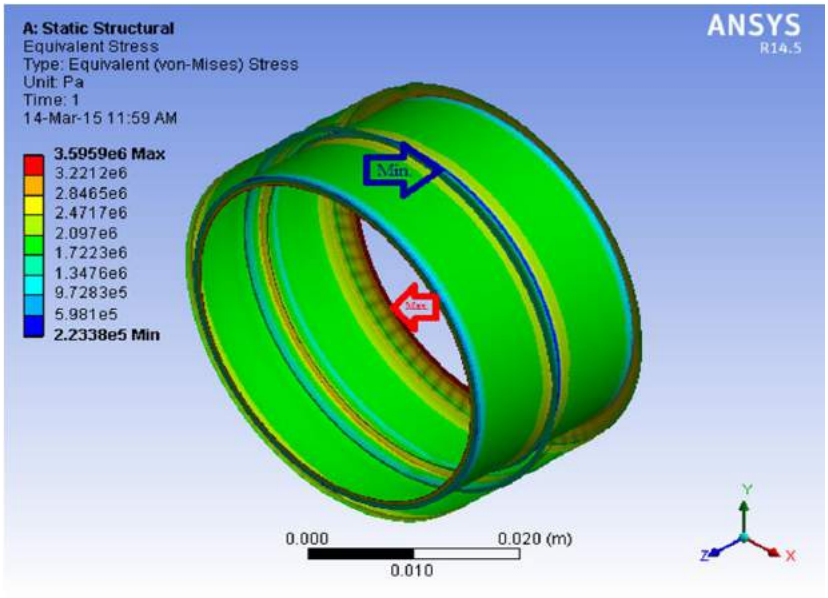

Figure 7-24 Equivalent stress rectangular cross section

7.2.3 Variation of Maximum Principal Stress

From the Figure 7-25, it can be observed that maximum principal stresses are plotted against the applied pressures. It can also be observed that maximum principal stresses are experienced in corrugated steel pipe having triangular corrugation. This may be due to the low young's modulus value and having sharp edges, stresses occurred in triangular corrugations. Similarly, the lowest maximum principal stress is found in corrugated steel pipe having circular corrugations. Moreover, if the pressure increases maximum principal stress also increases. The location of the maximum and minimum deformation is shown in Figure 7-26

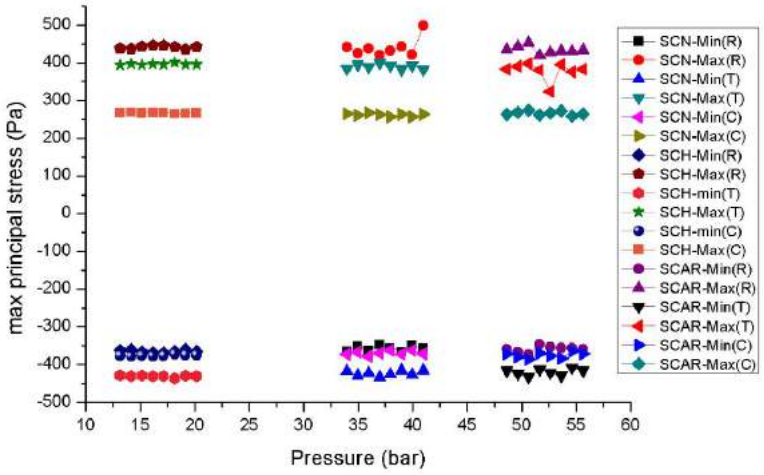

Figure 7-25 Maximum principal stress with respect to pressure

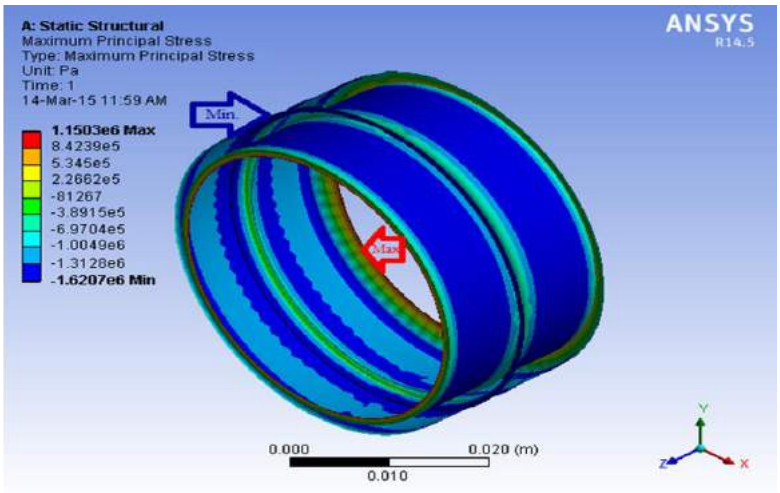

Figure 7-26 Maximum principal stress

7.2.4 Variation of Equivalent Elastic Strain

From the Figure 7-27, it can be observed that equivalent elastic strain are plotted against the applied pressures. It can also be observed that maximum equivalent elastic strain are experienced in corrugated steel pipe having triangular corrugation. This may be due to the low young's modulus value and having sharp edges, stresses occurred in triangular corrugations. Similarly, the lowest equivalent elastic strain is found in corrugated steel pipe having rectangular corrugations. Moreover, if the pressure increases equivalent elastic strain also increases. The location of the maximum and minimum deformation is shown in Figure 7-28

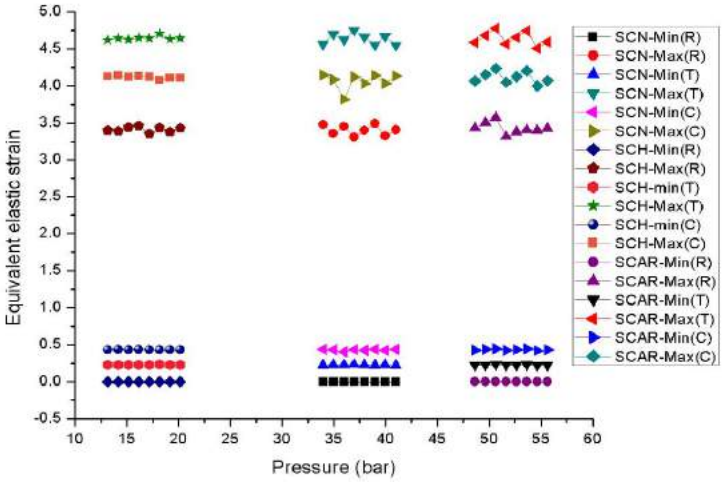

Figure 7-27 Equivalent elastic strain with respect to pressure

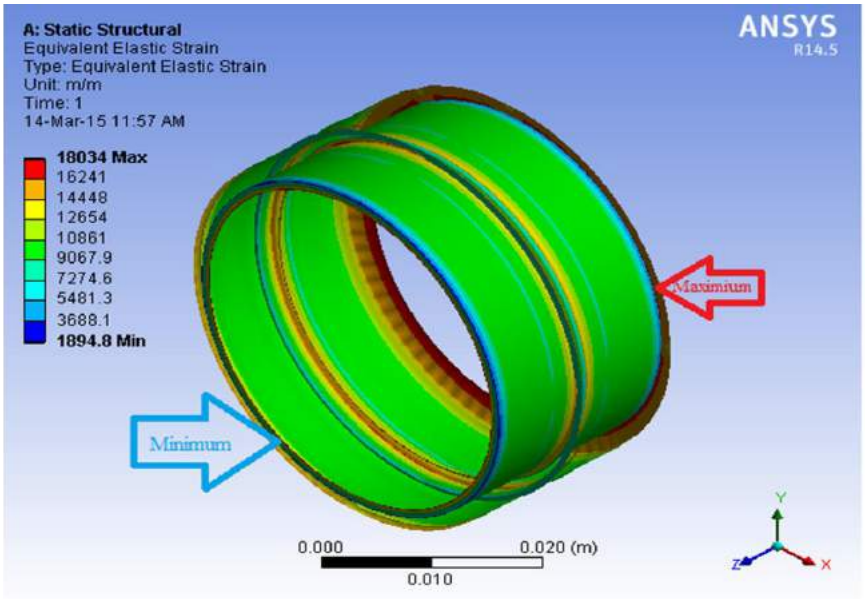

Figure 7-28 Equivalent elastic strain circular cross section

7.2.5 Variation of Maximum Principal Elastic Strain:

From the Figure 7-29, it can be observed that maximum principal elastic strain are plotted against the applied pressures. It can also be observed that maximum principal elastic strain are experienced in corrugated steel pipe having triangular corrugation. This may be due to the low young's modulus value and having sharp edges, stresses occurred in triangular corrugations. Similarly, the lowest maximum principal elastic strain is found in corrugated steel pipe having rectangular corrugations. Moreover, if the pressure increases maximum principal elastic strain also increases. The location of the maximum and minimum deformation is shown in Figure 7-30

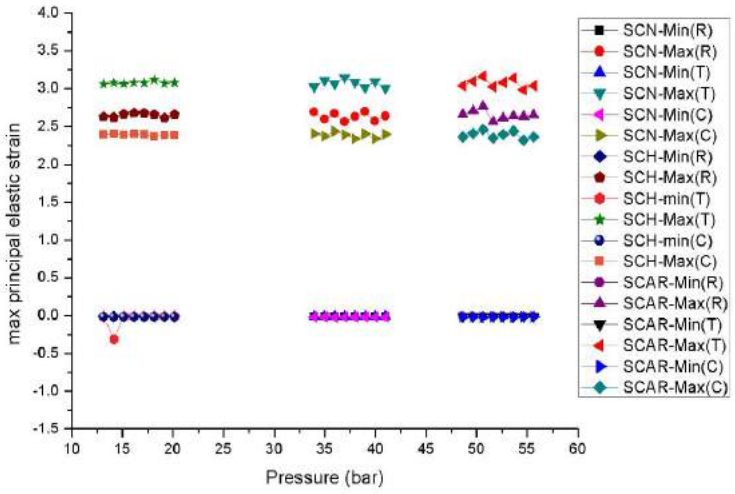

Figure 7-29 Maximum principal elastic strain with respect to pressure

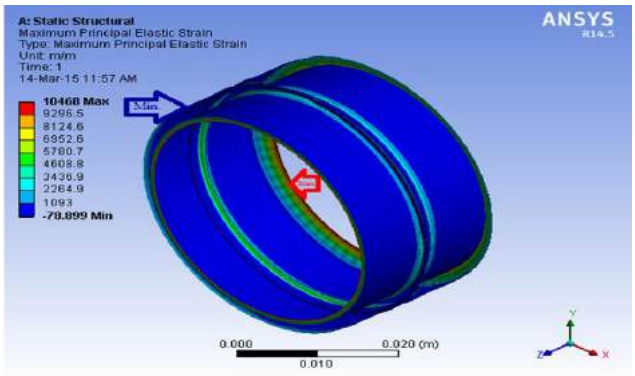

Figure 7-30 maximum principal elastic strain circular cross section

7.2.6 Variation of Shear Elastic Strain:

From the Figure 7-31, it can be observed that shear elastic strain is plotted against the applied pressure. It can also be observed that maximum elastic strain is experienced in corrugated steel pipe having triangular corrugation. This may be due to the sharp edges present in triangular corrugations. Similarly, the lowest elastic strain is found in corrugated steel pipe having circular corrugations which may be due to absence of sharp edges. The location of the maximum and minimum deformation is shown in Figure 7-32

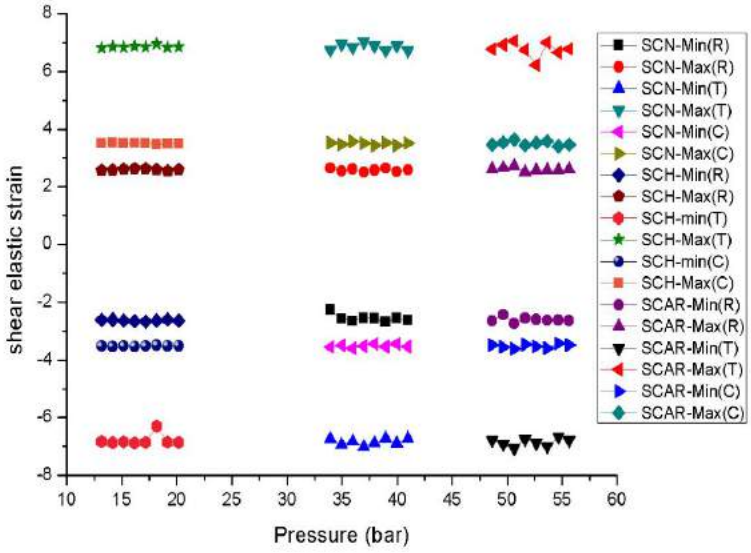

Figure 7-31 Shear elastic strain with respect to pressure

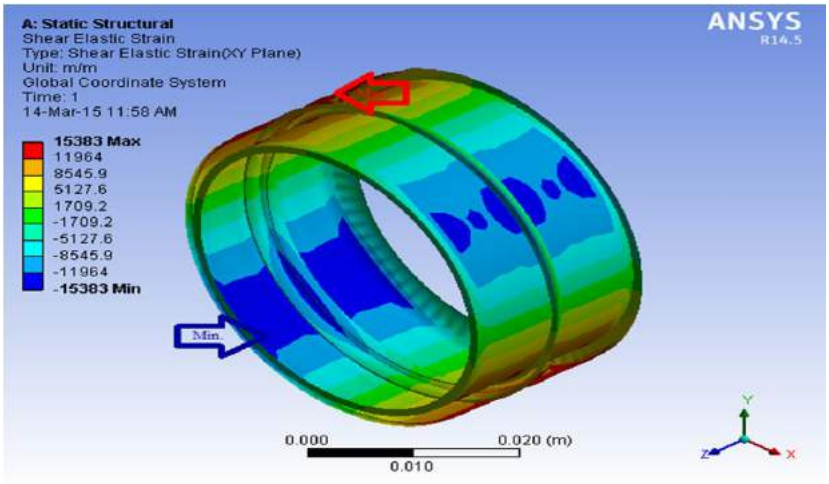

Figure 7-32 Shear elastic strain circular cross section

7.2.7 Variation of Maximum Shear Elastic Strain:

From the Figure 7-33, it can be observed that maximum shear elastic strain are plotted against the applied pressures. It can also be observed that maximum shear elastic strain is experienced in corrugated steel pipe having triangular corrugation. This may be due to the low young's modulus value and having sharp edges, stresses occurred in triangular corrugations. Similarly, the lowest shear elastic strain is found in corrugated steel pipe having circular corrugations. Moreover, if the pressure increases maximum shear elastic strain also increases in triangular corrugated pipe. The location of the maximum and minimum deformation is shown in Figure 7-34

.

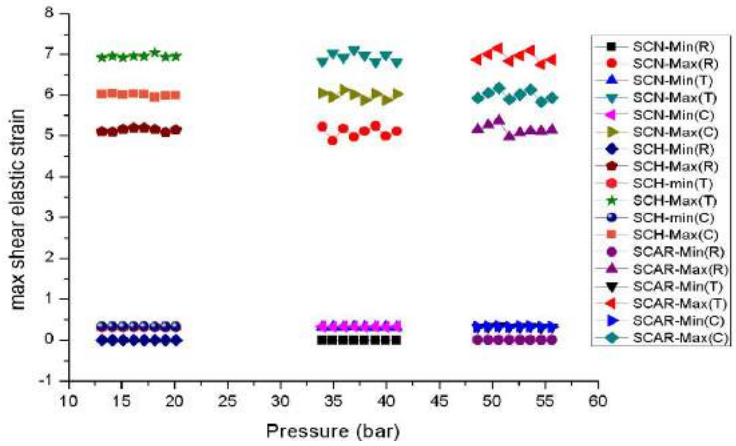

Figure 7-33 Maximum shear elastic strain with respect to pressure

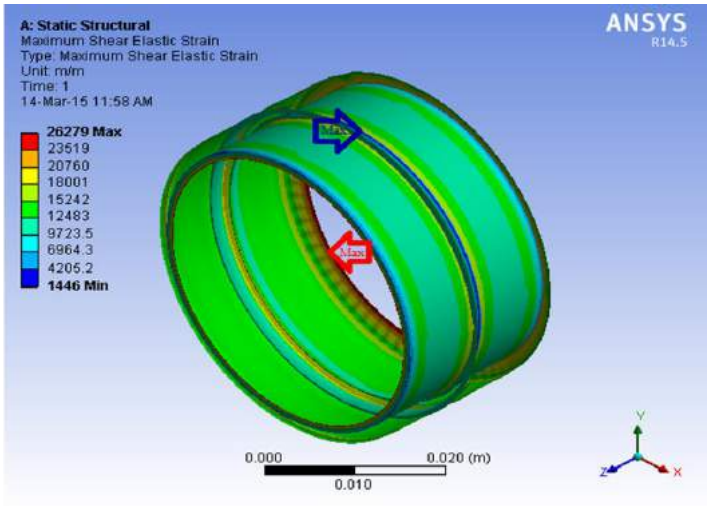

Figure 7-34 Maximum shear elastic strain circular cross section

7.2.8 Variation of Maximum Shear Stress:

From the Figure 7-35, it can be observed that maximum shear stress is plotted against the applied pressures. It can also be observed that maximum shear stresses are experienced in corrugated steel pipe having triangular corrugation. This may be due to the low young's modulus value and having sharp edges, stresses occurred in triangular corrugations. Similarly, the lowest maximum shear stress is found in corrugated steel pipe having rectangular corrugations. Moreover, if the pressure increases maximum shear stress also increases. The location of the maximum and minimum deformation is shown in Figure 7-36

.

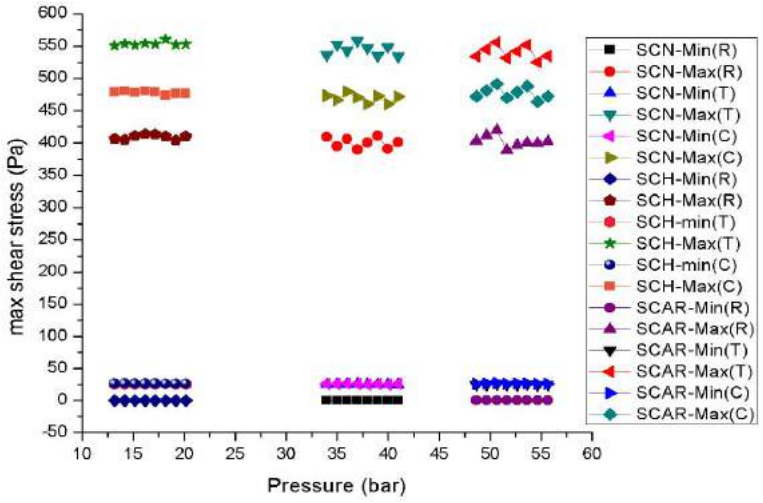

Figure 7-35 Maximum shear stress with respect to pressure

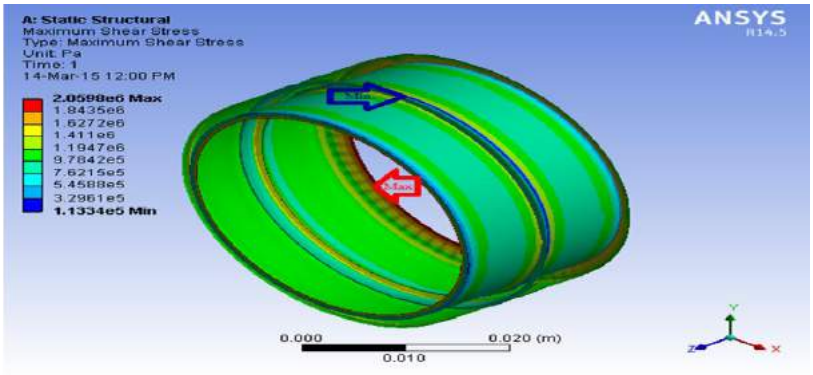

Figure 7-36 Maximum shear stress circular cross section

7.2.9 Variation of Strain Energy:

From the Figure 7-37, it can be observed that strain energy is plotted against the applied pressures. It can also be observed that maximum strain energy is experienced in corrugated steel pipe having triangular corrugation. This may be due to the low young's modulus value and having sharp edges, stresses occurred in triangular corrugations. Similarly, the lowest strain energy is found in corrugated steel pipe having circular corrugations. Moreover, if the pressure increases strain energy also increases. The location of the maximum and minimum deformation is shown in Figure 7-38

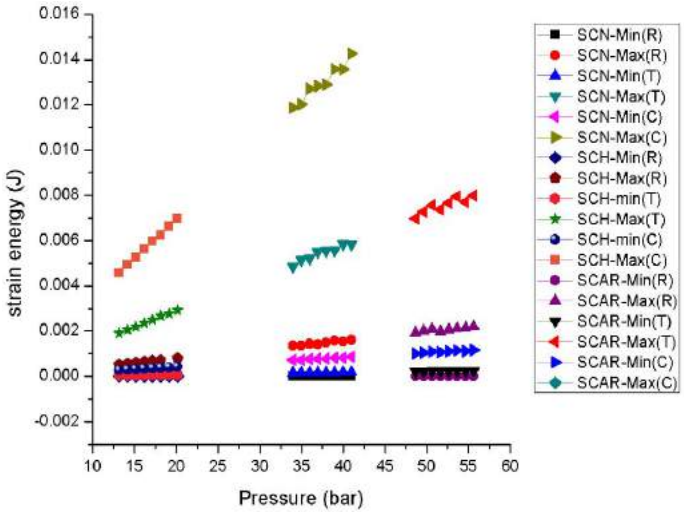

Figure 7-37 Strain energy with respect to pressure

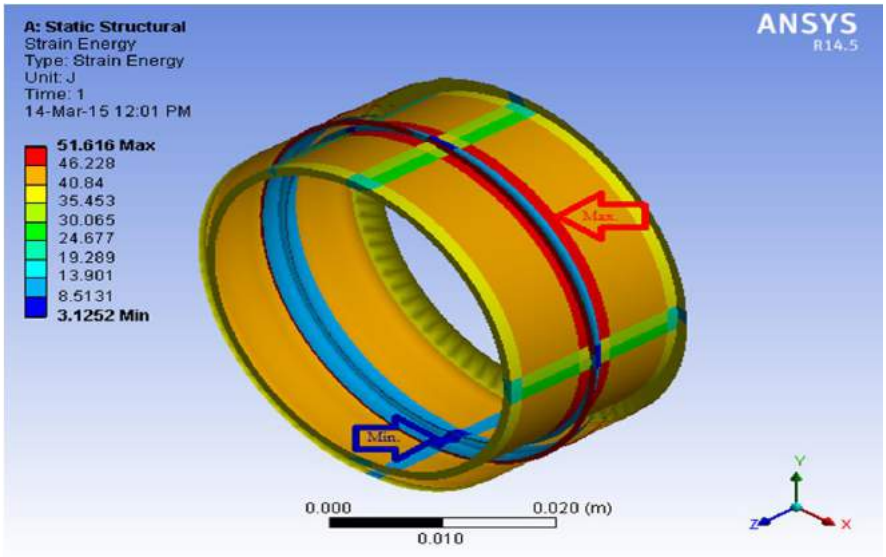

Figure 7-38 Strain energy circular cross section.

7.2.10 Variation of Total Deformation:

From the Figure 7-39, it can be observed that total deformation is plotted against the applied pressures. It can also be observed that maximum total deformation is experienced in corrugated steel pipe having triangular corrugation. This may be due to the low young's modulus value and having sharp edges, stresses occurred in rectangular corrugations. Similarly, the lowest strain energy is found in corrugated steel pipe having circular corrugations. Moreover, if the pressure increases total deformation also increases. The location of the maximum and minimum deformation is shown in Figure 7-40

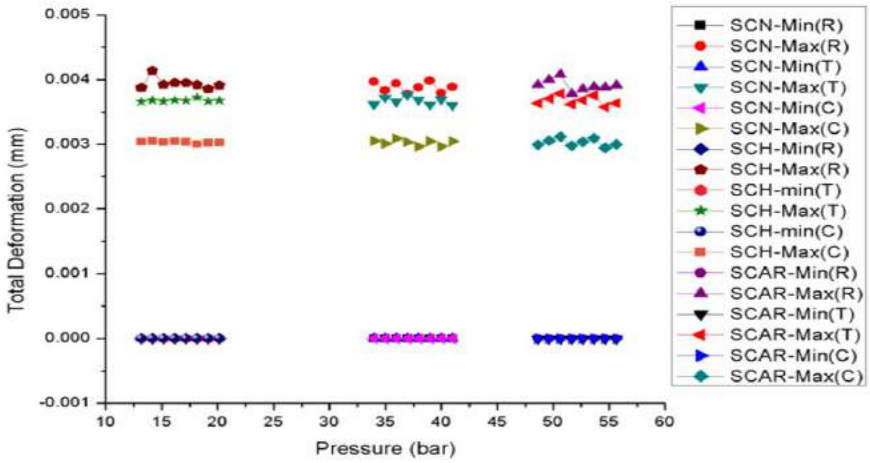

Figure 7-39 Total Deformation with respect to pressure

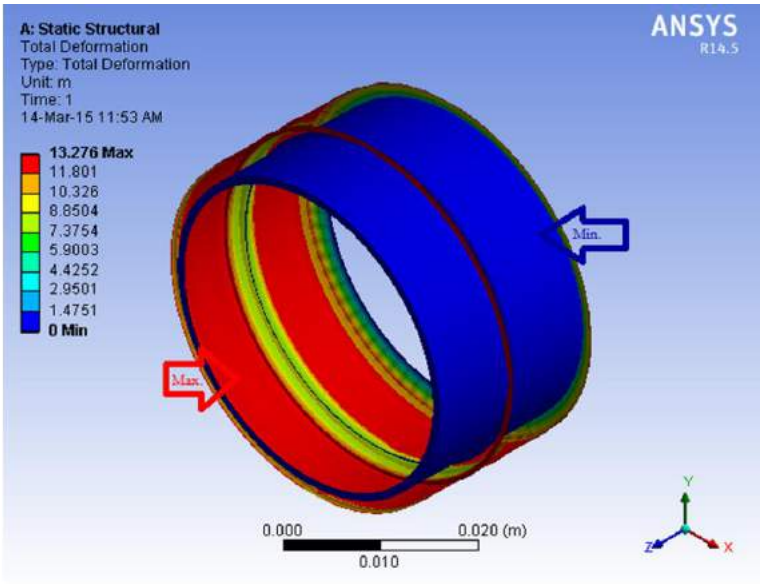

Figure 7-40 Total Deformation in Circular cross section

8 CONCLUSIONS

The main objective behind the study is the improvement of corrugations in stainless steel pipe which is present inside HTS cable, by passing different cryogenic fluids to cool and to overcome the issues that are occurring in power transmissions. To overcome the above problems a new and advanced technology known as superconductivity is introduced. In this proposed work the mechanical properties are analyzed. By keeping the temperature dependent properties like poison ratio, thermal conductivity, and young's modulus as constant the analysis is done. Till now the maximum stresses are occurring in triangular, rectangular followed by circular. So, circular corrugation is preferred and that in Supercritical Hydrogen (SCH).Maximum stresses that are occurring are very less in hydrogen while compared to the other gases. Almost in all the mechanical properties the C-type corrugation is having less stresses among the three corrugations. The maximum stresses are occurring in T-type, R-type followed by C-type. .Hence the C-type corrugation is preferred that to in SCH.

It is also concluded after studying the several research papers that the stresses that are occurring in HTS cables is still a challenging task and it may overcome by the use of different cryogenic fluids with different corrugations.

REFERENCES

[1] H. E.W.Lemmon, M.O.Mclinden, *NIST standa rd reference database, physical and chemical properties division", version7.0,beta, USA.* 2002, p. 30.

[2] T. Nakatsuka, A. Kikuchi, Y. Ozawa, and K. Ueda, "Research and development of superconducting cable in Super-ACE project," vol. 42, no. 2002, pp. 345–350, 2009.

[3] R. S. Dondapati, G. S. Member, and V. V Rao, "Pressure Drop and Heat Transfer Analysis of Long Length Internally Cooled HTS Cables," *IEEE Trans. Appiled Supercond.*, vol. 23, p. 5, 2013.

[4] D. Zhang, S. Dai, F. Zhang, T. Huang, Y. Wang, Y. Lin, Y. Teng, G. Zhang, L. Xiao, and L. Lin, "Design research on the conductor of 10kA class HTS DC power cable," *Cryogenics (Guildf).*, vol. 52, no. 12, pp. 725–729, Dec. 2012.

[5] F. Grilli, R. Brambilla, F. Sirois, A. Stenvall, and S. Memiaghe, "Development of a three-dimensional finite-element model for high-temperature superconductors based on the H-formulation," *Cryogenics (Guildf).*, vol. 53, pp. 142–147, Jan. 2013.

[6] M. Oomen, W. Herkert, D. Bayer, P. Kummeth, W. Nick, and T. Arndt, "Manufacturing and test of 2G-HTS coils for rotating machines: Challenges, conductor requirements, realization," *Phys. C Supercond.*, vol. 482, pp. 111–118, Nov. 2012.

[7] F. Schmidt and A. Allais, "SUPERCONDUCTING CABLES FOR POWER TRANSMISSION APPLICATIONS – A REVIEW," pp. 232–237.

[8] S. C. Kim, D. W. Ha, S. S. Oh, I. Y. Han, C. E. Bruzek, J. G. Oh, and H. S. Sohn, "Study on thermo-mechanical treatment in fabrication of Bi2212/Ag HTS wire," *Cryogenics (Guildf).*, vol. 47, no. 7–8, pp. 437–441, Jul. 2007.

[9] T. Famakinwa, Q. M. Chen, and S. Yamaguchi, "3D finite element analysis of eddy current loss of HTS tapes – External field analysis," *Phys. C Supercond.*, vol. 459, no. 1–2, pp. 18–23, Aug. 2007.

[10] T. Hemmi, N. Yanagi, G. Bansal, K. Seo, K. Takahata, and T. Mito, "Electromagnetic behavior of HTS coils in persistent current operations," *Fusion Eng. Des.*, vol. 81, no. 20–22, pp. 2463–2466, Nov. 2006.

[11] H. J. Kim, D. S. Kwag, Y. S. Kim, and S. H. Kim, "Electrical characteristics of high-Tc superconducting mini-model cable under mechanical stresses in liquid nitrogen," *Cryogenics (Guildf).*, vol. 45, no. 1, pp. 45–50, Jan. 2005.

[12] M. Furuse, S. Fuchino, and N. Higuchi, "Investigation of structure of superconducting power transmission cables with LN2 counter-flow cooling," *Phys. C Supercond.*, vol. 386, pp. 474–479, Apr. 2003.

[13] C. Suzuki, K. Goto, T. Saitoh, and T. Nakatsuka, "Strain properties of transposed segment conductors for a transmission cable," *Phys. C Supercond.*, vol. 392–396, pp. 1186–1191, Oct. 2003.

[14] T. Masuda, T. Kato, H. Yumura, M. Hirose, S. Isojima, S. Honjo, K. Matsuo, T. Mimura, and Y. Takahashi, "Experimental results of a 30 m, 3-core HTSC cable," *Phys. C Supercond.*, vol. 372–376, pp. 1555–1559, Aug. 2002.

[15] Erdogan Kiran, Pablo G.Debenedetti and Cor J.Peters, " Supercritical Fluids: Fundamental and Applications", Series E: Applied Sciences-Vol. 366

[16] Erdogen Kiran, Johana M.H. Levelt Sengers, "Seprcritical Fluids Fundamentals for Application", NATO ASI Series, Vol.273(1993)

[17] E.W.Lemmon, M.O.Mclinden, and M.L.Huber," NIST standard reference database, physical and chemical properties division", version 7.0,beta,7/30/02, USA.

[18] R. Wesche, a Anghel, B. Jakob, G. Pasztor, R. Schindler, and G. Vécsey, "Design of superconducting power cables," *Cryogenics (Guildf).*, vol. 39, no. 9, pp. 767–775, Sep. 1999.

[19] J. A. Demko, J. W. Lue, M. J. Gouge, J. P. Stovall, U. Sinha, and R. L. Hughey, "Practical AC Loss and Thermal Considerations for HTS Power Transmission Cable Systems," vol. I, no. 1, 2001.

[20] A. Posada, Y. I. Kim, and V. Manousiouthakis, "On conduction-cooling of a high-temperature superconducting cable," *Cryogenics (Guildf).*, vol. 46, no. 6, pp. 458–467, Jun. 2006.

APPENDIX

Mechanical analysis of a corrugated steel pipe (SS316LN) containing different cryogenic fluids

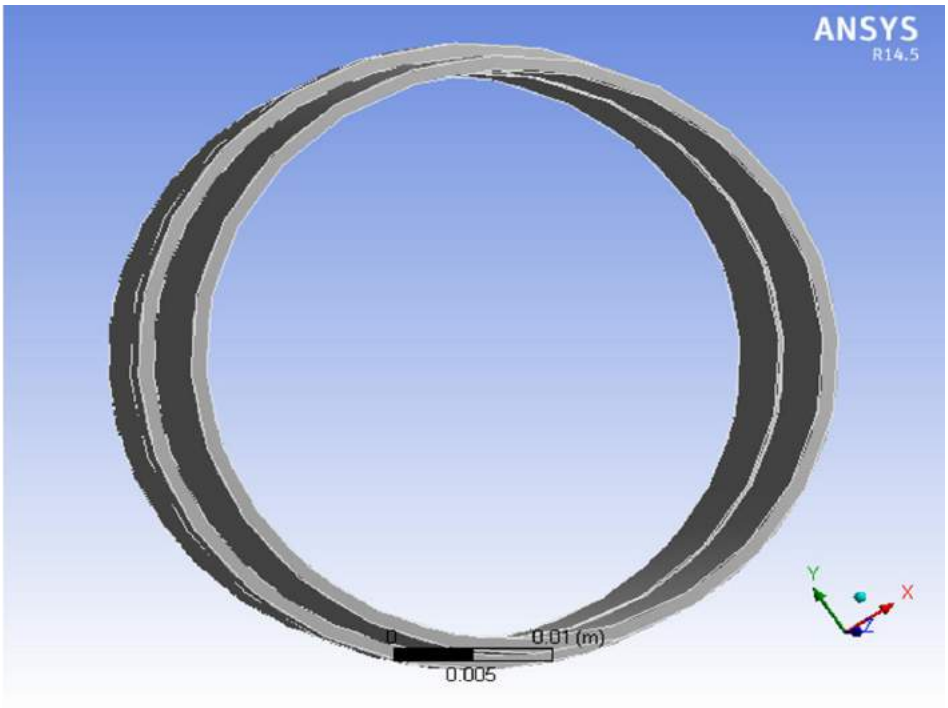

Units

TABLE 1

Unit System	Metric (m, kg, N, s, V, A) Degrees rad/s Celsius
Angle	Degrees
Rotational Velocity	rad/s
Temperature	Celsius

Model (A4)

Geometry

TABLE 2

Model (A4) > Geometry

Object Name	*Geometry*
State	Fully Defined
Definition	
Source	G:\dissertation2\final geometries\RECTANGLE\NITROGEN\csp33_files\dp0\SYS\DM\SYS.agdb
Type	Design Modeler
Length Unit	Millimeters
Element Control	Program Controlled
Display Style	Body Color
Bounding Box	
Length X	4.4e-002 m
Length Y	4.4e-002 m
Length Z	2.1e-002 m
Properties	
Volume	2.8463e-006 m³
Mass	2.2343e-002 kg
Scale Factor Value	1.
Statistics	
Bodies	1
Active Bodies	1
Nodes	37981

Elements	18952
Mesh Metric	None
Basic Geometry Options	
Parameters	Yes
Parameter Key	DS
Attributes	No
Named Selections	No
Material Properties	No
Advanced Geometry Options	
Use Associativity	Yes
Coordinate Systems	No
Reader Mode Saves Updated File	No
Use Instances	Yes
Smart CAD Update	No
Attach File Via Temp File	Yes
Temporary Directory	C:\Users\User\AppData\Roaming\Ansys\v145
Analysis Type	3-D
Decompose	Yes

Disjoint Geometry	
Enclosure and Symmetry Processing	Yes

TABLE 3

Model (A4) > Geometry > Parts

Object Name	*Solid*
State	Meshed
Graphics Properties	
Visible	Yes
Transparency	1
Definition	
Suppressed	No
Stiffness Behavior	Flexible
Coordinate System	Default Coordinate System
Reference Temperature	By Environment
Material	
Assignment	Structural Steel
Nonlinear Effects	Yes
Thermal Strain Effects	Yes
Bounding Box	
Length X	4.4e-002 m
Length Y	4.4e-002 m
Length Z	2.1e-002 m
Properties	
Volume	2.8463e-006 m³
Mass	2.2343e-002 kg
Centroid X	1.1508e-018 m

Centroid Y	-2.479e-018 m
Centroid Z	1.05e-002 m
Moment of Inertia Ip1	5.4713e-006 kg·m²
Moment of Inertia Ip2	5.4713e-006 kg·m²
Moment of Inertia Ip3	9.3886e-006 kg·m²
Statistics	
Nodes	37981
Elements	18952
Mesh Metric	None

Coordinate Systems

TABLE 4

Model (A4) > Coordinate Systems > Coordinate System

Object Name	*Global Coordinate System*
State	Fully Defined
Definition	
Type	Cartesian
Coordinate System ID	0.
Origin	
Origin X	0. m
Origin Y	0. m
Origin Z	0. m
Directional Vectors	
X Axis Data	[1. 0. 0.]
Y Axis Data	[0. 1. 0.]
Z Axis Data	[0. 0. 1.]

Mesh

TABLE 5

Model (A4) > Mesh

Object Name	*Mesh*
State	Solved
Defaults	
Physics Preference	Mechanical
Relevance	0
Sizing	
Use Advanced Size Function	Off
Relevance Center	Fine
Element Size	Default
Initial Size Seed	Active Assembly
Smoothing	Medium
Transition	Fast
Span Angle Center	Coarse
Minimum Edge Length	0.125660 m
Inflation	
Use Automatic Inflation	None
Inflation Option	Smooth Transition
Transition Ratio	0.272
Maximum Layers	5
Growth Rate	1.2
Inflation Algorithm	Pre
View Advanced Options	No
Patch Conforming Options	
Triangle Surface Mesher	Program Controlled
Advanced	
Shape Checking	Standard Mechanical
Element Midside Nodes	Program Controlled
Straight Sided Elements	No

Number of Retries	Default (4)
Extra Retries For Assembly	Yes
Rigid Body Behavior	Dimensionally Reduced
Mesh Morphing	Disabled
Defeaturing	
Pinch Tolerance	Please Define
Generate Pinch on Refresh	No
Automatic Mesh Based Defeaturing	On
Defeaturing Tolerance	Default
Statistics	
Nodes	37981
Elements	18952
Mesh Metric	None

Static Structural (A5)

TABLE 6

Model (A4) > Analysis

Object Name	*Static Structural (A5)*
State	Solved
Definition	
Physics Type	Structural
Analysis Type	Static Structural
Solver Target	Mechanical APDL
Options	
Environment Temperature	22. °C
Generate Input Only	No

TABLE 7

Model (A4) > Static Structural (A5) > Analysis Settings

Object Name	*Analysis Settings*
State	Fully Defined
Step Controls	

Number Of Steps	1.
Current Step Number	1.
Step End Time	1. s
Auto Time Stepping	Program Controlled
Solver Controls	
Solver Type	Program Controlled
Weak Springs	Program Controlled
Large Deflection	Off
Inertia Relief	Off
Restart Controls	
Generate Restart Points	Program Controlled
Retain Files After Full Solve	No
Nonlinear Controls	
Force Convergence	Program Controlled
Moment Convergence	Program Controlled
Displacement Convergence	Program Controlled
Rotation Convergence	Program Controlled
Line Search	Program Controlled
Stabilization	Off
Output Controls	
Stress	Yes

Strain	Yes
Nodal Forces	No
Contact Miscellaneous	No
General Miscellaneous	No
Store Results At	All Time Points
Max Number of Result Sets	Program Controlled
Analysis Data Management	
Solver Files Directory	G:\dissertation2\final geometries\RECTANGLE\NITROGEN\csp33_files\dp0\SYS\MECH\
Future Analysis	None
Scratch Solver Files Directory	
Save MAPDL db	No
Delete Unneeded Files	Yes
Nonlinear Solution	No
Solver Units	Active System
Solver Unit System	mks

TABLE 8

Model (A4) > Static Structural (A5) > Loads

Object Name	*Pressure 2*	*Fixed Support*
State	Fully Defined	
Scope		
Scoping Method	Geometry Selection	
Geometry	3 Faces	7 Faces
Definition		
Type	Pressure	Fixed Support
Define By	Normal To	
Magnitude	3.3958e+006 Pa (ramped)	
Suppressed	No	

FIGURE 1

Model (A4) > Static Structural (A5) > Pressure 2

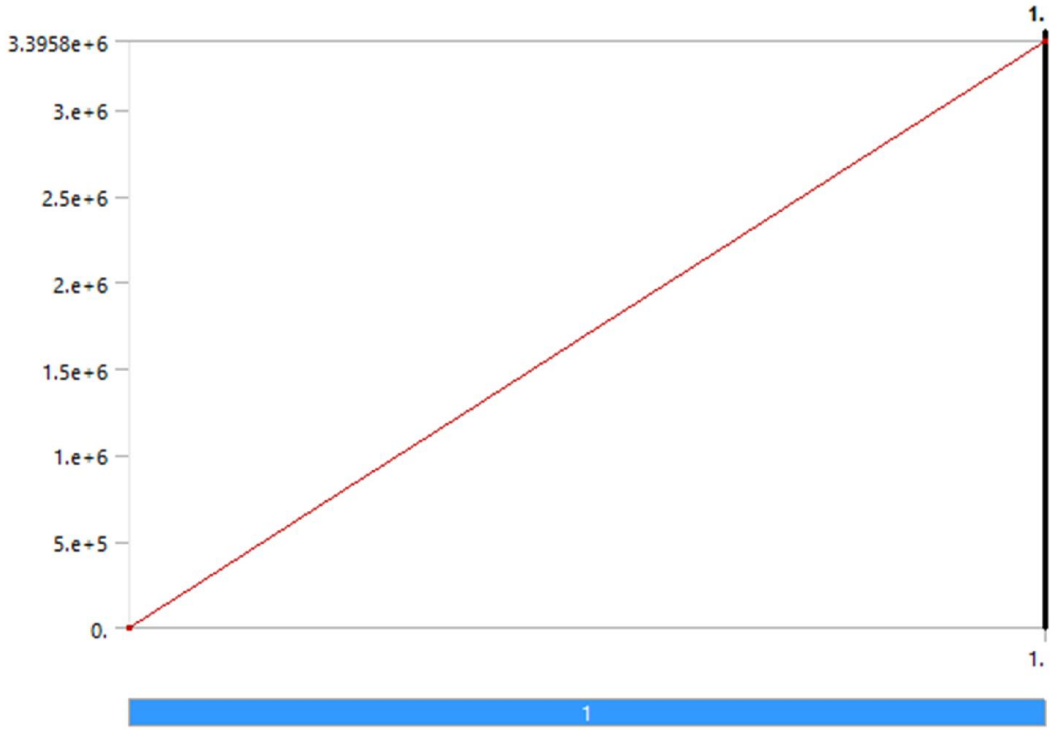

Solution (A6) **TABLE 9**

Model (A4) > Static Structural (A5) > Solution

Object Name	*Solution (A6)*
State	Solved
Adaptive Mesh Refinement	
Max Refinement Loops	1.
Refinement Depth	2.
Information	
Status	Done

TABLE 10

Model (A4) > Static Structural (A5) > Solution (A6) > Solution Information

Object Name	*Solution Information*
State	Solved
Solution Information	
Solution Output	Solver Output
Newton-Rap son Residuals	0
Update Interval	2.5 s
Display Points	All
FE Connection Visibility	
Activate Visibility	Yes
Display	All FE Connectors
Draw Connections Attached To	All Nodes
Line Color	Connection Type
Visible on Results	No
Line Thickness	Single
Display Type	Lines

TABLE 11

Model (A4) > Static Structural (A5) > Solution (A6) > Results

Object Name	*Total Deformation*	*Maximum Principal Elastic Strain*	*Directional Deformation*	*Equivalent Elastic Strain*	*Maximum Shear Elastic Strain*

State	Solved				
Scope					
Scoping Method	Geometry Selection				
Geometry	All Bodies				
Definition					
Type	Total Deformation	Maximum Principal Elastic Strain	Directional Deformation	Equivalent Elastic Strain	Maximum Shear Elastic Strain
By	Time				
Display Time	Last				
Calculate Time History	Yes				
Identifier					
Suppressed	No				
Orientation			X Axis		
Coordinate System			Global Coordinate System		
Results					
Minimum	0. m	-56.612 m/m	-20.877 m	7.7017 m/m	3.1602 m/m
Maximum	24.818 m	16811 m/m	20.805 m	21728 m/m	32611 m/m
Information					
Time	1. s				
Load Step	1				
Substep	1				
Iteration Number	1				
Integration Point Results					
Display Option		Averaged		Averaged	

TABLE 12

Model (A4) > Static Structural (A5) > Solution (A6) > Results

Object Name	*Equivalent Stress*	*Maximum Principal Stress*	*Maximum Shear Stress*	*Shear Stress*	*Shear Elastic Strain*
State	Solved				
Scope					
Scoping Method	Geometry Selection				
Geometry	All Bodies				
Definition					
Type	Equivalent (von-Misses) Stress	Maximum Principal Stress	Maximum Shear Stress	Shear Stress	Shear Elastic Strain
By	Time				
Display Time	Last				
Calculate Time History	Yes				
Identifier					
Suppressed	No				
Orientation				XY Plane	
Coordinate System				Global Coordinate System	
Integration Point Results					
Display Option	Averaged				
Results					
Minimum	454.4 Pa	-2.2803e+006 Pa	247.96 Pa	-1.3076e+006 Pa	-16664 m/m
Maximum	4.4327e+006 Pa	2.7571e+006 Pa	2.5588e+006 Pa	1.2946e+006 Pa	16499 m/m

Information	
Time	1. s
Load Step	1
Substep	1
Iteration Number	1

TABLE 13

Model (A4) > Static Structural (A5) > Solution (A6) > Results

Object Name	*Strain Energy*
State	Solved
Scope	
Scoping Method	Geometry Selection
Geometry	All Bodies
Definition	
Type	Strain Energy
By	Time
Display Time	Last
Calculate Time History	Yes
Identifier	
Suppressed	No
Results	
Minimum	1.7304e-002 J
Maximum	8.5155 J
Information	
Time	1. s
Load Step	1
Substep	1
Iteration Number	1

Material Data

Structural Steel **TABLE 14**

Structural Steel > Constants

Density	7850 kg m^-3
Coefficient of Thermal Expansion	1.2e-005 C^-1
Specific Heat	434 J kg^-1 C^-1
Thermal Conductivity	60.5 W m^-1 C^-1
Resistivity	1.7e-007 ohm m

TABLE 15

Structural Steel > Compressive Ultimate Strength

Compressive Ultimate Strength Pa
0

TABLE 16

Structural Steel > Compressive Yield Strength

Compressive Yield Strength Pa
2.5e+008

TABLE 17

Structural Steel > Tensile Yield Strength

Tensile Yield Strength Pa
2.5e+008

TABLE 18

Structural Steel > Tensile Ultimate Strength

Tensile Ultimate Strength Pa
4.6e+008

TABLE 19

Structural Steel > Isotropic Secant Coefficient of Thermal Expansion

Reference Temperature C
22

TABLE 20

Structural Steel > Alternating Stress Mean Stress

Alternating Stress Pa	Cycles	Mean Stress Pa
3.999e+009	10	0
2.827e+009	20	0
1.896e+009	50	0
1.413e+009	100	0
1.069e+009	200	0
4.41e+008	2000	0
2.62e+008	10000	0
2.14e+008	20000	0
1.38e+008	1.e+005	0
1.14e+008	2.e+005	0
8.62e+007	1.e+006	0

TABLE 21

Structural Steel > Strain-Life Parameters

Strength Coefficient Pa	Strength Exponent	Ductility Coefficient	Ductility Exponent	Cyclic Strength Coefficient Pa	Cyclic Strain Hardening Exponent
9.2e+008	-0.106	0.213	-0.47	1.e+009	0.2

TABLE 22

Structural Steel > Isotropic Elasticity

Temperature C	Young's Modulus Pa	Poisson's Ratio	Bulk Modulus Pa	Shear Modulus Pa
126	204.01	0.3	170.01	78.464
126.1	204	0.3	170	78.462
126.2	203.99	0.3	169.99	78.459
126.3	203.99	0.3	169.99	78.456
126.4	203.98	0.3	169.98	78.453
126.5	203.97	0.3	169.98	78.451
126.6	203.96	0.3	169.97	78.448

126.7	203.96	0.3	169.96	78.445
126.8	203.95	0.3	169.96	78.443
126.9	203.94	0.3	169.95	78.44
127	203.94	0.3	169.95	78.437
127.1	203.93	0.3	169.94	78.434
127.2	203.92	0.3	169.94	78.432
127.3	203.91	0.3	169.93	78.429
127.4	203.91	0.3	169.92	78.426
127.5	203.9	0.3	169.92	78.423
127.6	203.89	0.3	169.91	78.421
127.7	203.89	0.3	169.91	78.418
127.8	203.88	0.3	169.9	78.415
127.9	203.87	0.3	169.89	78.412
128	203.86	0.3	169.89	78.41
128.1	203.86	0.3	169.88	78.407
128.2	203.85	0.3	169.88	78.404
128.3	203.84	0.3	169.87	78.401
128.4	203.84	0.3	169.86	78.399
128.5	203.83	0.3	169.86	78.396
128.6	203.82	0.3	169.85	78.393
128.7	203.81	0.3	169.85	78.39
128.8	203.81	0.3	169.84	78.388
128.9	203.8	0.3	169.83	78.385
129	203.79	0.3	169.83	78.382
129.1	203.79	0.3	169.82	78.379
129.2	203.78	0.3	169.82	78.376
129.3	203.77	0.3	169.81	78.374
129.4	203.76	0.3	169.8	78.371
129.5	203.76	0.3	169.8	78.368
129.6	203.75	0.3	169.79	78.365
129.7	203.74	0.3	169.79	78.363

129.8	203.74	0.3	169.78	78.36
129.9	203.73	0.3	169.77	78.357
130	203.72	0.3	169.77	78.354
130.1	203.71	0.3	169.76	78.351
130.2	203.71	0.3	169.76	78.349
130.3	203.7	0.3	169.75	78.346
130.4	203.69	0.3	169.74	78.343
130.5	203.68	0.3	169.74	78.34
130.6	203.68	0.3	169.73	78.338
130.7	203.67	0.3	169.73	78.335
130.8	203.66	0.3	169.72	78.332
130.9	203.66	0.3	169.71	78.329
131	203.65	0.3	169.71	78.326
131.1	203.64	0.3	169.7	78.324
131.2	203.63	0.3	169.7	78.321
131.3	203.63	0.3	169.69	78.318
131.4	203.62	0.3	169.68	78.315
131.5	203.61	0.3	169.68	78.312
131.6	203.61	0.3	169.67	78.31
131.7	203.6	0.3	169.66	78.307
131.8	203.59	0.3	169.66	78.304
131.9	203.58	0.3	169.65	78.301
132	203.58	0.3	169.65	78.298
132.1	203.57	0.3	169.64	78.296
132.2	203.56	0.3	169.63	78.293
132.3	203.55	0.3	169.63	78.29
132.4	203.55	0.3	169.62	78.287
132.5	203.54	0.3	169.62	78.284
132.6	203.53	0.3	169.61	78.282
132.7	203.52	0.3	169.6	78.279
132.8	203.52	0.3	169.6	78.276

132.9	203.51	0.3	169.59	78.273
133	203.5	0.3	169.59	78.27
133.1	203.5	0.3	169.58	78.268
133.2	203.49	0.3	169.57	78.265
133.3	203.48	0.3	169.57	78.262
133.4	203.47	0.3	169.56	78.259
133.5	203.47	0.3	169.56	78.256
133.6	203.46	0.3	169.55	78.253
133.7	203.45	0.3	169.54	78.251
133.8	203.44	0.3	169.54	78.248
133.9	203.44	0.3	169.53	78.245
134	203.43	0.3	169.52	78.242
134.1	203.42	0.3	169.52	78.239
134.2	203.41	0.3	169.51	78.236
134.3	203.41	0.3	169.51	78.234
134.4	203.4	0.3	169.5	78.231
134.5	203.39	0.3	169.49	78.228
134.6	203.39	0.3	169.49	78.225
134.7	203.38	0.3	169.48	78.222
134.8	203.37	0.3	169.48	78.22
134.9	203.36	0.3	169.47	78.217
135	203.36	0.3	169.46	78.214
135.1	203.35	0.3	169.46	78.211
135.2	203.34	0.3	169.45	78.208
135.3	203.33	0.3	169.44	78.205
135.4	203.33	0.3	169.44	78.202

TABLE 23

Structural Steel > Isotropic Relative Permeability

Relative Permeability
10000